RESEARCH ARTICLE Journal of Daylighting 9 (2022) 97-116 doi:10.15627/jd.2022.7

ISSN 2383-8701

Journal of Daylighting

Journal homepage: https://solarlits.com/jd

Impact of Different Shading Devices on Daylight Performance and Visual Comfort of A Four Opening Sides' Reading Room In Rasht

Banafsheh Dabaj,[a] Morteza Rahbar,[*,b] Bahereh Vojdani Fakhr[c]

[a] Master of Energy and Architecture, Pars University of Architecture and Art, Tehran, Iran

[b] School of Architecture and Environmental Design, Iran University of Science and Technology, Tehran, Iran

[c] Department of Art and Architecture, Tarbiat Modares University, Tehran, Iran

Article info

Article history:
Received 25 February 2022
Revised 22 April 2022
Accepted 3 May 2022
Published online 30 June 2022

Keywords:
Daylighting
Discomfort glare
Reading room
Shading system

Abstract

Daylighting has become an essential feature in libraries since it can boost productivity, well-being, and energy savings. It is crucial to prevent discomfort glare irritation while maintaining the quality of view, and daylight demands. This study compares four different shading systems on all fronts of a reading room. Shading devices include a Perforated Solar Screen (PSS), besides three Venetian Blinds typologies (exterior, interior, and exterior integrated with overhangs) are generated considering various parameters. The 60-min time step for an entire year is used to find out the worst dates for glare analysis in different positions for Rasht, Iran. The findings of Daylight Autonomy (DA), Useful Daylight Illuminance (UDI), Daylight Glare Probability (DGP), and Quality of View (QV) depict that PSS is ineffective at glare reduction but is adequate for annual metrics and view quality. Moreover, Venetian Blinds in every three typologies are sufficient to deal with glare problems on most dates, despite differences in their characteristics being reported. Annual metrics and Quality of View in these cases, depending on variables, are changeable.

© 2022 The Author(s). Published by solarlits.com. This is an open access article under the CC BY license (https://creativecommons.org/licenses/by/4.0/).

1. Introduction

Humans have always sought to learn and comprehend throughout their lives. As time goes by, realizing the importance of this issue, learning and studying facilities such as schools, colleges, libraries, and study halls have been built. Adequate daylight quantity and visual comfort are becoming increasingly crucial in such spaces [1] since natural light provides positive psychological, mental, and physiological effects on building occupants. It has the potential to impact the user's productivity, wellbeing, circadian rhythms, mood, alertness, etc. [2-5]. As a renewable source, the available daylight also can reduce artificial lighting using diffusing light from the sky and ambient Environment [6,7]. Nevertheless, excessive sunlight remains problematic in terms of glare and undesirable visual discomfort [8]. Avoiding glare is considered a critical aspect of addressing visual discomfort to do essential visual work in high daylight availability and clear sky.

Glare can be defined as the sensation caused by luminance in the field of view that is too great that the eye cannot adapt to it. Therefore, discomfort or loss in visual performance and visibility are occurred [9]. It is commonly divided into two categories: disability glare and discomfort glare. Disability glare makes a person unable to see specific objects in a field of view, while discomfort glare produces discomfort without necessarily influencing visual performance and visibility. This phenomenon can occur either when the amount of light reaching the observer's eyes is excessive or when an observer experiences a too wide range of luminance in a given visual field. The extreme contrast between illuminated and dark parts of the visual field causes a progressive decline in visual performance. As a result, it leads to premature eye fatigue, and in the following, it also causes a feeling of discomfort or other symptoms such as headaches [10].

Visual comfort in the indoor environment has been a substantial factor in learning and is recognized to improve the educational process [11]. In addition, the positive impact of the quality of view on wellbeing [12] and eye health [13] is reported. Reading rooms are often used during the day. Hence the challenges caused by sunlight are essential to be addressed in the design. In daylighting design, to successfully obtain the profits of utilizing natural light sources in buildings, discomfort glare should be prevented [14]. Due to the need for people's long-term presence in these places, the lack of glare control causes adverse effects on users,

*Corresponding author.
banafsheh.dabaj@pu.ac.ir (B. Dabaj)
rahbarm@iust.ac.ir (M. Rahbar)
Bahereh.vojdani@modares.ac.ir (B. V. Fakhr)

2383-8701/© 2022 The Author(s). Published by solarlits.com. This is an open access article under the CC BY license (https://creativecommons.org/licenses/by/4.0/).

Nomenclature

ASE	*Annual Sunlit Exposure*
CIE	*Co1nn1ission Inteniationale de l'Eclairage*
DA	*Daylight Autono1ny*
DGP	*Daylight Glare Probability*
LEED	*Leadership in Energy and Environ1nental Design*
QV	*Quality of View*
UDI	*Useful Daylight Ilh11ninance*
WWR	*Window-to-wall ratio*
E	*Illuminance, Lux*
$L_{s,i}$	*The luminance of the i-th glare source, cd/1112*
P_i	*Position index of the i-th glare source, -*
$\omega_{s,i}$	*The solid angle of the i-th glare source based on the viewing position of the observer, sr*
t	*Time, hour*
E_v	*Ve11ical illu1ninance at eye level, Lux*
wf	*Weighting factor*

inefficiency, or absence. Optimal glare control by placing barriers in or blocking sunlight might adversely affect views to the outside and/or daylight indicators. Therefore, it is critical to identify effective shading design factors which ultimately lead to a comprehensive design and maximal response to the demands of the user's needs. A fundamental goal for architects, building engineers, and designers has been to maximize the valuable daylight in interior spaces as much as possible [15].

Due to the high relative humidity, the moderate climate often is foggy and cloudy. This study has selected a moderate climate since the beneficial use of daylight on sunny days is essential. For maximum use of daylight, the windows are located in four directions modeled on the article's hypotheses. Although large glasses in facades allow natural light and the outdoors view in buildings, they are accompanied by visual discomfort [2]. Therefore, it is difficult to control the glare in a clear sky in such spaces. The main innovation of this research is the assessment of suchlike buildings that are more exposed to glare and have not been studied before. There are countless study halls and libraries that are glazed in all directions to maximize the use of daylight, such as Sainte-Geneviève Library [16], Central Library Oodi in Helsinki [17], Suzzallo-Allen Library [18], and so on.

It is necessary to consider the glare that reaches the user's eyes from different directions in such places. This study intends to evaluate the performance of shading to reduce glare in different users' fields of view by performing simulations. The purpose of the present article is to investigate different shadings performance and identify their effective parameters on daylight performance, quality of view, and diminishing glare caused by natural daylight in a reading room with daylight coming in from all sides. Despite having windows on all four sides, the main research question is to what extent the shadings are able to manage the discomfort glare and deliver beneficial daylight into the room. Another question that can be addressed is to what extent each shading parameter is effective in enhancing visual comfort factors. It can be determined which of the shading has the most potential for keeping the user from being exposed to the glare phenomena over more dates in different directions. This paper's results indicate the significant effects of shading on glare control and the impact of its types on visual comfort and daylight efficiency. The focus on visual comfort has been investigated to maximize the internal environmental conditions for the user's presence.

2. Background

Architectural design with massive windows has become a trend in recent decades, resulting in high energy consumption. It also has a substantial impact on daylighting and occupant visual comfort.

Many studies have been carried out on daylight design [19-23], daylight performance [24-28], quality of view [29-31], and strategies used to reduce glare [32-36]. Although each study has researched a specific topic, their goals have been increasing visual comfort and reducing energy consumption or using some methods to make reviews more accurate in achieving these goals. For instance, Xue, P et al. [37], confirmed that daylight performance improves by increasing Window-to-Wall Ratio (WWR). Furthermore, sunshades have a positive effect on reducing the cooling load, even with high WWR. Yuan Fang and Soolyeon Cho [38] presented a parametric design for energy-saving and daylight efficiency for three different climates. They concluded that among the studied variables, the width and length of the skylight are the most significant variables.

Some scholars have focused on building facades to reduce energy consumption and improve daylight performance [3,39]. As a result of a study by Lu, S et al. [40], it turns out that the optimized curve facade significantly improves the daylight performance. Seasonal and daily changes in solar positions and sky conditions prompted researchers to study the dynamic facade's effect on daylight efficiency. Hosseini, S. M et al. [15] compared the simple, two-dimensional-shape-change-façade (2D-SCF) and three-dimensional-shape-change-façade (3D-SCF) aimed at visual comfort and reducing glare, which resulted in 3D-SCF has a better performance to achieve this purpose. Origami patterns inspired designers to do research related to this context [41,42]. A hexagonal responsive skin as a dynamic shading system was examined to provide visual comfort by Tabadkani et al. [43] which indicates that based on the user preference, using a proposed timing pattern on a responsive skin can increase daylight reception and provide shading with controlling glare.

Recent studies have highlighted the effect of blinds and louvers on improving comfort and energy performance [44-46]. Daniel Uribe et al. [47] examined the impact of control strategies for moving curved perforated louvers to attain an acceptable level of visual comfort and minimize office space's total energy consumption in different climatic conditions. Samadi, S et al. [48] proved that applying kinetic shading systems in optimal states enhances indoor daylight efficiency. A study by Santos L et al. [49], the Lasy_S system installed in the air gap of the double-pane window and LightLouver placed inside the room was simulated to better light performance at the back of the room. The findings confirmed that the LightLouver system performs better in diffusing, creating a low-contrast environment, and avoiding glare. At the same time, the Lasy_S prevents excessive daylight in addition to the better light-directing performance at the back of the room. As a result of a study on the material parameters of Venetian blinds with the aim of energy savings in residential buildings, Solar Reflectance and Transmittance are introduced as two key parameters [50]. A study was conducted on the effect of External Venetian blinds on nearly zero-energy buildings for the different climates in China. Results indicate that WWR, Shape of the

2383-8701/© 2022 The Author(s). Published by solarlits.com. This is an open access article under the CC BY license (https://creativecommons.org/licenses/by/4.0/).

building, and Slat Angle are linearly associated with the shading performance [51].

Several studies noted the importance of human physiological responses to discomfort glare [52-54]. Research by Hamedani et al. [55] which focused on this issue, claims that during the study, the eye fixation rate increases under high glare conditions while the blinking rate is low. Follow to Rosenfield's advice [56]; eye blinking is a natural mechanism in the human body to keep a healthy ocular surface and clarity of vision; the frequency of a lower blinking can lead to faster evaporation of tears and possibly dry eyes. Furthermore, to get rid of discomfort glare caused by daylight, the user increases the probability of a curtain being operated and uses artificial lighting [57]. Hence energy consumption rises.

All studies have proved the crucial of enhancing beneficial daylight, both in terms of energy reduction and visual comfort, that determine the accuracy and sensitivity of researchers to this context. This issue inspires authors to research in this field. Various strategies and shading systems were discussed in the background, whereas most of the simulations investigated one side of the building (usually the southern front for the northern hemisphere and the northern front for the southern hemisphere). They did not take into account all direction openings. Among all the previous scenarios, not only discomfort glare conditions throughout the year have not been seriously assessed, but also, they have typically considered predetermined dates in which the building was exposed to glare according to the state of the sun in winter or summer. Also, they have not cared about the shadings' performance potential on most glare dates. Besides, the impact of shadings on different directions that are simultaneously exposed to glare has not been addressed. The superiority of shading performance, particularly the performance of PSS to counteract glare compared to different Venetian Blinds typologies, is not specified. The present study intends to fill the mentioned gaps.

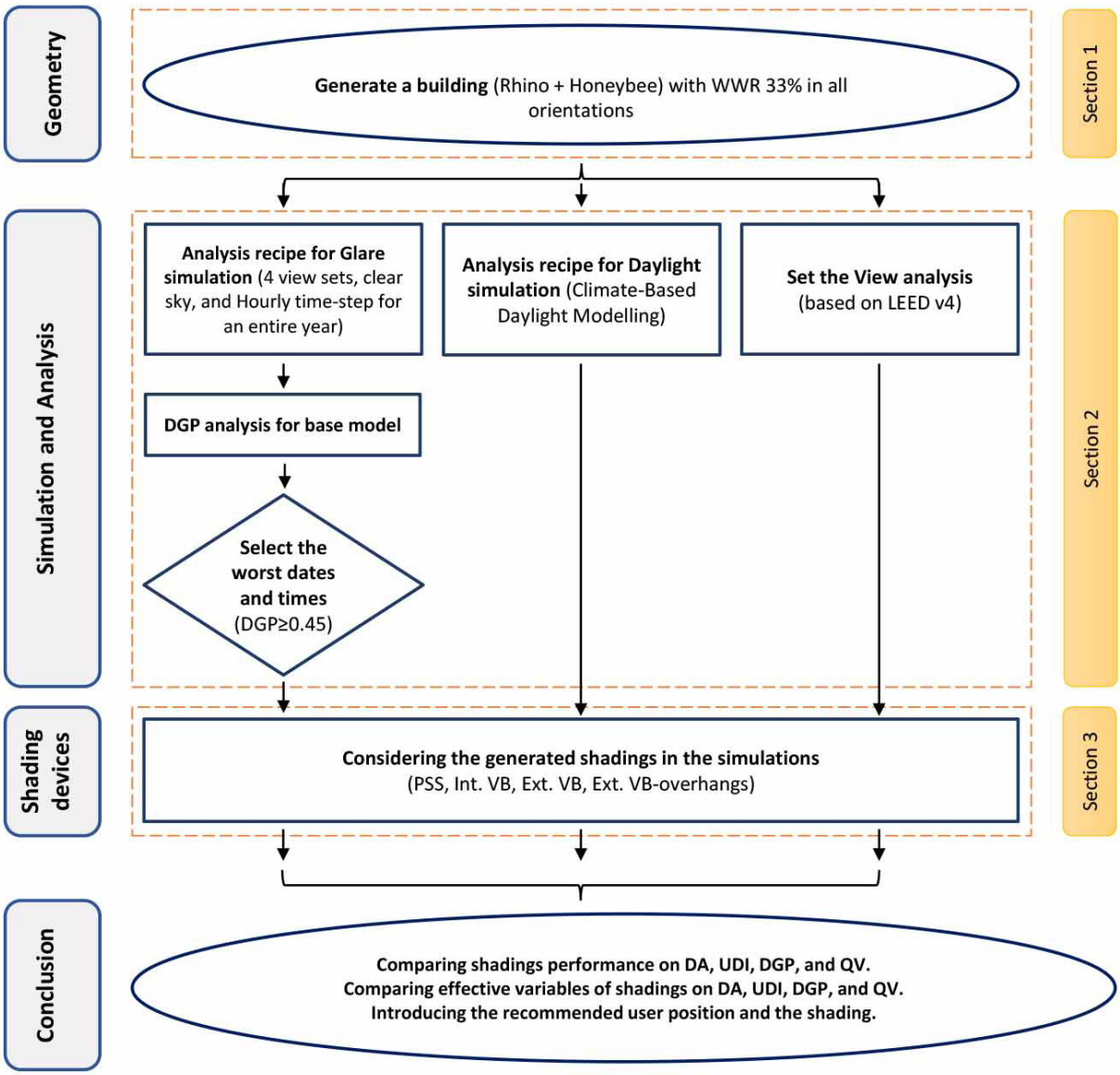

Fig. 1. Illustrating flow chart.

2383-8701/© 2022 The Author(s). Published by solarlits.com. This is an open access article under the CC BY license (https://creativecommons.org/licenses/by/4.0/).

3. Methodology

The research approach's overall process for obtaining both visual comfort and daylight efficiency is shown in Fig. 1. The present study uses simulation tools based on Daysim/Radiance engines; Grasshopper plugins Ladybug (Version 0.0.68) and Honeybee (Version 0.0.65), and goes through several stages, where the first step is to prepare the building geometry. Invariable parameters are clarified in section 3.1. After the geometry is set up, the next step is to simulate the model, once without considering the shading and the subsequent times with different shading devices, to find how the shadings operate. The selected climate, indicators, and simulation settings are described in detail in the Second Section. Besides, the view analysis setting based on LEED v4 is included to respond to how much shadings affect the Quality of View. Various shading systems and their variable parameters are presented in section 3.3. Finally, the following sections interpret the simulation output results and discussions. The method for determining the shade success rate is obtained by comparing the maximum number of dates in which the glare reduction occurred to the number of glare dates in the base model. It should be noted how much the indicator has grown dramatically from the base model to compare the shading performance in terms of daylight efficiency.

3.1. Set up for reading room model

A reading room represents the interior space with 8m (length), 5m (depth), and 3m (height). The room is modeled by Rhino software. It has windows with a 33% Window-to-Wall Ratio (WWR) on all fronts. Since various WWRs have been used in different studies [58-60], in this article, approximately the average of these intervals is assumed. For the east and west fronts, three windows besides the north and south, four windows with 0.80m sill height, and 2m height are considered as the room has a rectangular plan and elongation in the east-west axis. Windows have a visual transmittance equal to 80%, and the surfaces' reflectances are the following; floor (%20), ceiling (%70), and wall (%50) [61]. The analysis plane is placed 0.75m above the floor (a typical desk height), and the size of the gride test is set to be 0.50 m. Since the door's location affects neither daylight simulation nor glare analysis, the door may be placed anywhere on the solid parts of the walls. Therefore, its position has not been displayed (Fig. 2).

3.2. Simulation settings, selected criteria, and the weather file

As stated by Reinhard, CF et al. [62], dynamic daylight performance metrics are based on timed series of illuminances in buildings, which is considered the entire year, the quantity and character of daily and seasonal instabilities of daylight for a given building, and rare meteorological events. Since numerous articles have used Daylight Autonomy (DA) and Useful Daylight Illuminance (UDI) for such spaces [63-65], in the present study, DA and UDI were selected as two climate-based metrics for the case evaluation. DA is defined as the percentage of occupied hours of the year in which the minimum illuminance threshold is met only by daylight [66,67]. It is formulated in Eq. (1) [68]

$$DA = \frac{\sum_i (wf_i \cdot t_i)}{\sum_i t_i} \in [0,1] \tag{1}$$

with $$wf_i = \begin{cases} 1 & if \quad E_{Daylight} \geq E_{limit} \\ 0 & if \quad E_{Daylight} < E_{limit} \end{cases},$$

where:

t_i is each occupied hour in a year, wf_i is a weighting factor, $E_{Daylight}$ is the horizontal illuminance at a given point caused by only daylight, and E_{limit} is the illuminance limit value.

UDI represents the percentage of time where the daylight level is useful for the occupants. It is categorized into three bins; too dark or underlit (<100 lux), usable daylight (100-2000 lux), and too bright or overlit with the possibility of glare (>2000 lux) [66]. Its formulation is shown in Eq. (2) [68]:

$$UDI = \frac{\sum_i wf_i \cdot t_i}{\sum_i t_i} \in [0,1] \tag{2}$$

$$UDI_{Overlit} \quad \text{with} \quad wf_i = \begin{cases} 1 & \text{if} \quad E_{Daylight} > E_{Upper\ limit} \\ 0 & \text{if} \quad E_{Daylight} \leq E_{Upper\ limit} \end{cases}$$

$$UDI_{Useful} \quad \text{with} \quad wf_i = \begin{cases} 1 & \text{if} \quad E_{Lower\ limit} \leq E_{Daylight} \leq E_{Upper\ limit} \\ 0 & \text{if} \quad E_{Daylight} < E_{Lower\ limit} \vee E_{Daylight} > E_{Upper\ limit} \end{cases}$$

$$UDI_{Underlit} \quad \text{with} \quad wf_i = \begin{cases} 1 & \text{if} \quad E_{Daylight} < E_{Lower\ limit} \\ 0 & \text{if} \quad E_{Daylight} \geq E_{Lower\ limit} \end{cases}$$

UDI in the range of 100-2000 lux is evaluated in this research. According to the British Standards Institution [69], the illuminance threshold for educational spaces is 300-500 lux.

Table 1. Profile of the studied region.

City	Köppen-Geiger classification	Location	Average daylight (hour)	Average sunshine (days)	Average cloud cover (%)	sun position variability (°)
Rasht (Iran)	Csa	37.2682° N, 49.5891° E	Jun: 14.7h Dec: 9.6h	Jul: 20.7 Sep: 12.5	Feb: 40 Jun: 15	21 Jun: 73.3 21 Dec: 20.91

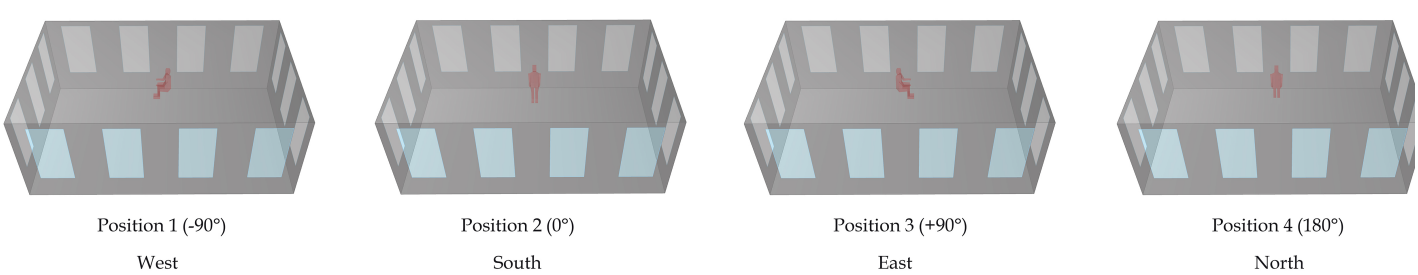

Fig. 2. Positions to analyze DGP.

2383-8701/© 2022 The Author(s). Published by solarlits.com. This is an open access article under the CC BY license (https://creativecommons.org/licenses/by/4.0/).

Therefore, 300 lux is considered the illuminance threshold for DA. According to [70,71], the target level for UDI should be above 50%, and [72] considers 50% of the floor area for DA.

The most adequate and powerful metric for analyzing the appearance of discomfort glare is the Discomfort Glare Probability (DGP) [66]. Also, it shows more relevance to the user's response in terms of glare perception. DGP is a short-term, local, one-tailed index assessing glare [73] and is divided into 4 different intervals: imperceptible glare (DGP<0.35), perceptible glare (0.35≤DGP<0.4), disturbing glare (0.4≤DGP<0.45), and intolerable glare (DGP≥0.45) [74]. The DGP is formulated in Eq. (3) [74]:

$$DGP = 5.87 \cdot 10^{-5} E_v + 0.0918 \log\left(1 + \sum_i \frac{L_{s,i}^2 \cdot \omega_{s,i}}{E_v^{1.87} \cdot P_i^2}\right) + 0.16 \quad (3)$$

where E_v is the vertical eye illuminance (Lux), L_s is the luminance of source (cd/m^2), ω_s is the solid angle of the source (sr), and P is the position index.

In the present study, Rasht is selected as a moderate climate. It is located in the north of Iran at 37.2682° N latitude and 49.5891° E longitude. The average daylight hours in the summer solstice (21 June) are 14.7 hours and in the winter solstice (21 December) is 9.6 hours. The sun is at an angle of 73.3° and 20.91° on the mentioned dates, respectively. On average, there are 20.7 days of sunshine in July in the best condition, and in the worst case, there are only 12.5 days in September. The largest cloud cover is about 40% in February, and the lowest amount is around 15% in June. Climatic and geographical information is summarized in Table 1. Although Rasht has different sky conditions throughout the year, and this probably affects the amount of achieving annual daylight, in this article, the Sunny with Sun sky type was required in Honeybee Generate CIE Standard Sky for glare simulation since the clear sky is more likely to glare risks [55]. As Fig. 2 shows, the sitting position facing the windows in four directions included -90°(West), 0°(South), 90°(East), and 180° (North), was considered to check the shadings function in each direction. Henceforth, in this study, for brevity, these positions are named P1, P2, P3, and P4, respectively. The simulations were performed one-hour time step in 12 months of the year, 30 days of the month,

Table 2. Variables of shading systems.

Shading device	Perforated Solar Screen (PSS)	Interior Venetian Blinds	Exterior Venetian Blinds	Exterior Venetian Blinds integrated with overhangs
Perforation ratio (%)	W-E: 27.47, 37.32, 48.75 N-S: 28.55, 38.87, 50.77	_	_	_
Distance to glass (m)	0.05, 0.1, 0.15, 0.2	0.05, 0.1, 0.15, 0.2	0.05, 0.1, 0.15, 0.2	0.05, 0.1, 0.15, 0.2
Slats' depth (m)	_	0.04, 0.08, 0.12	0.04, 0.08, 0.12	0.04, 0.08, 0.12
Slats' angle (°)	_	-60, -45, -30 ,30 ,45, 60	-60, -45, -30 ,30 ,45, 60	-60, -45, -30 ,30 ,45, 60

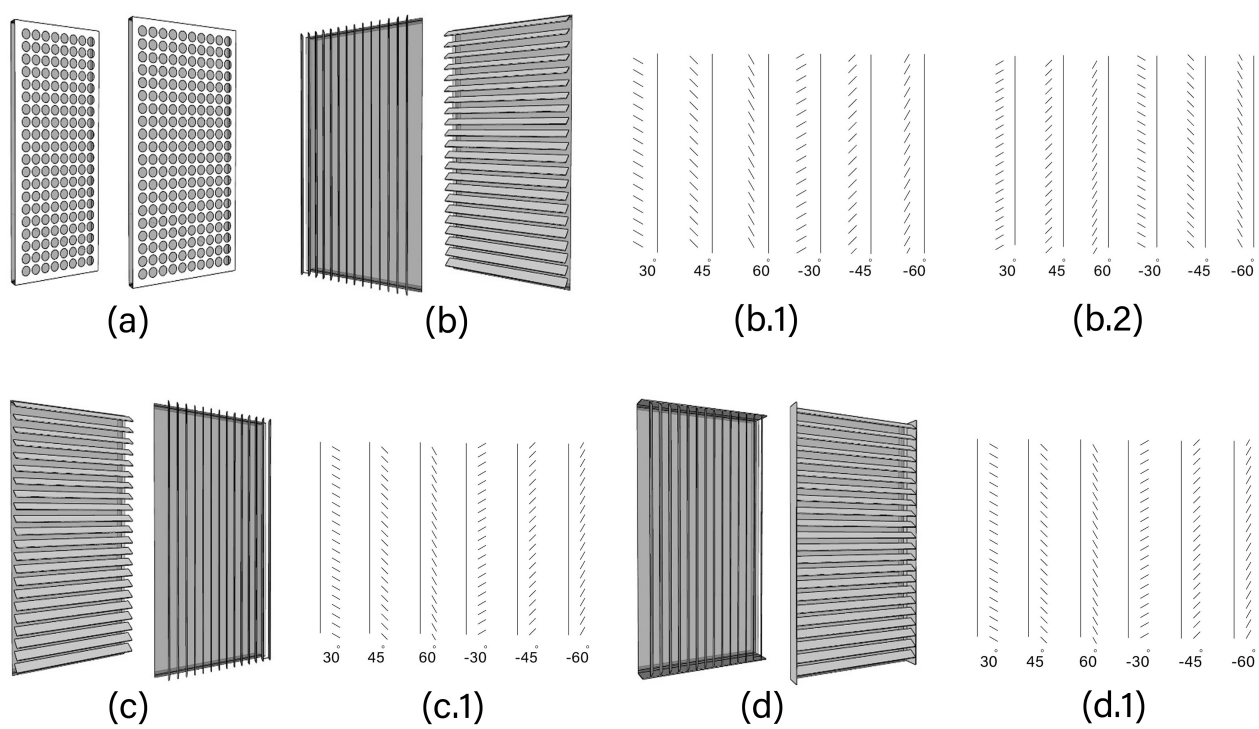

Fig. 3. Shading devices characteristic. (**a**) Perforated Solar Screen, (**b**): Interior Venetian Blinds, (**b.1**) Side view of an Interior Venetian Blind with horizontal slats, (**b.2**) Top view of an Interior Venetian Blind with vertical slats, (**c**): Exterior Venetian Blinds, (**c.1**) Side view of an Exterior Venetian Blind with horizontal slats (or top view of the blind with vertical slats), (**d**) Exterior Venetian Blinds integrated with overhangs (**d.1**) Section of an Exterior Venetian Blinds integrated with overhangs with horizontal slats (or Section of the blind with vertical slats).

2383-8701/© 2022 The Author(s). Published by solarlits.com. This is an open access article under the CC BY license (https://creativecommons.org/licenses/by/4.0/).

and from 7 am to 6 pm to find the worst dates (DGP≥0.45) for all mentioned positions.

3.3. Complex building shadings

Four different shading devices are placed on windows, as Fig. 3 shows; (a): Perforated Solar Screen (PSS), (b): Interior Venetian Blinds (Int. VB), (c): Exterior Venetian Blinds (Ext. VB), and (d): Exterior Venetian Blinds integrated with overhangs (Ext. VB-overhangs).

The PSS has circular apertures in the form of an 8\times20 matrix for east and west windows (0.83m width \times 2m height), in addition to a 10\times20 matrix for the north and south windows (1m width \times 2m height) (Fig. 3(a)). The PSS is considered as a single opaque surface without thickness with %80 reflectance and zero specularity and modeled parametrically by Grasshopper. In this case, the variable parameters are the perforation ratio and the PSS distance to glass. When the circle radiuses are 3, 3.5, and 4 cm, the perforation ratio for east and west windows are 27.47%, 37.32%, 48.75%, and for north and south windows are 28.55%, 38.87%, 50.77%, respectively. The PSS's distance to glass is considered 5, 10, 15, and 20 cm.

The second shading device is placed on the interior side of the glazing. The default blinds material considered has 65% solar

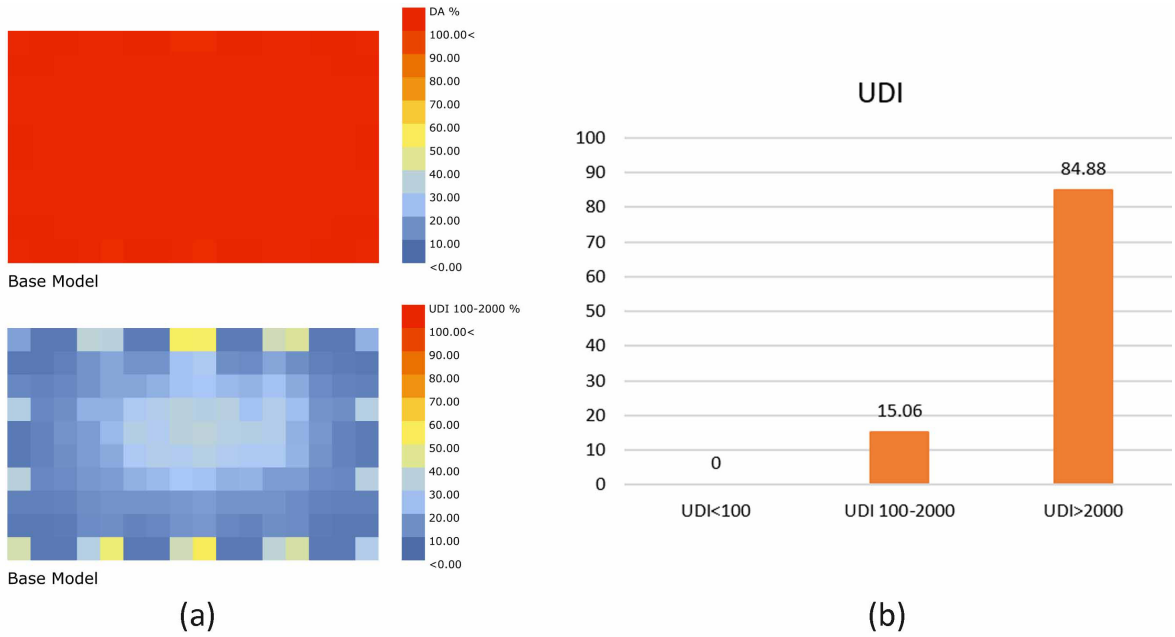

Fig. 4. Simulation outputs visualization of the base model. (**a**) The DA and UDI are based on percentages. (**b**) UDI intervals.

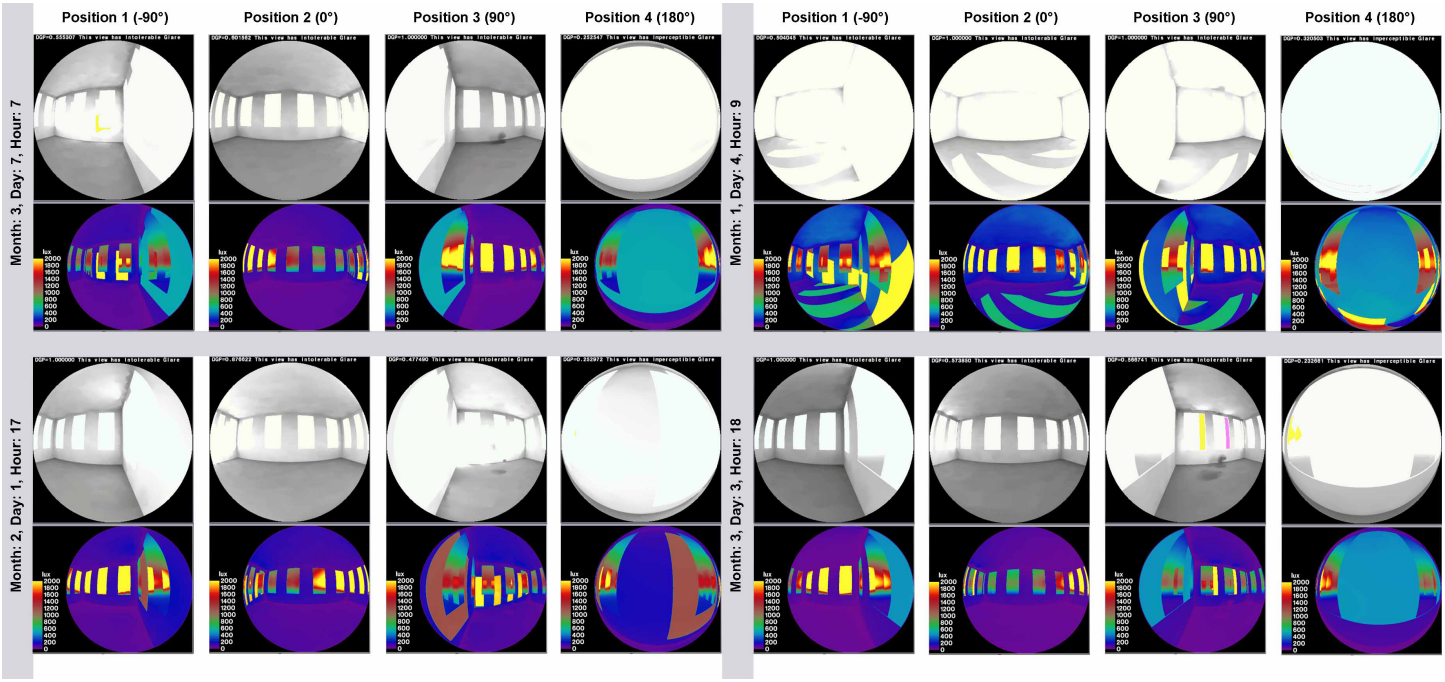

Fig. 5. Some of the worst dates and times of discomfort glare.

2383-8701/© 2022 The Author(s). Published by solarlits.com. This is an open access article under the CC BY license (https://creativecommons.org/licenses/by/4.0/).

reflectance, zero transmittance, 90% emittance, and a thickness of 0.25 mm. The shades are assumed to be always on. The variable parameters in the Interior Venetian Blinds (Int. VB) are the angle of slats in degrees such as -60°, -45°, -30°, 30°, 45°, and 60°; the blinds' distance to glass included 5, 10, 15, and 20 cm, and the depth of slats functioning as 4, 8, and 12 cm. It should be noted that, as Fig. 3(b) demonstrates, for the east and west fronts, the slats are on the vertical axis. In contrast, the slats are supposed to be on the horizontal axis on the north and south fronts.

Exterior Venetian Blinds (Ext. VB) have the same characteristics as the second one, but it is placed outside the room. Fig. 3(c) shows some differences between the slat's angle.

The last model is Exterior Venetian Blinds integrated with overhangs (Ext. VB-overhangs). The only difference between this case and the previous one is the screens on the window's sides. As Fig. 3(d) shows, for vertical axis blinds, the fixed screens are horizontally at the top and bottom of the window, while for the horizontal axis, the fixed screens are located vertically to the right and left. The depth of the blind slats changes the depth of the screen. All parameters are summarized in Table 2.

4. Results

The selected metrics are required to compare each shading device's performance to the base model for satisfying visual comfort and daylight efficiency. The results are described in the five sections, and the findings obtained from their comparison are described in the following discussion section.

4.1. Base model

As mentioned before, the base model has been evaluated regardless of the shading. The daylight simulation outputs are illustrated in Fig. 4. It proves that the average DA is 99.15% which can be interpreted that the DA in 100% of the test points receives daylight more than the threshold (300 lux). Figure 4(b), which is presented the UDI intervals, indicates that it is only about 15% in the range of 100-2000 lux, and the UDI blue areas in Fig. 4(a) receive daylight of approximately 85% more than 2000 lux, which are prone to glare and overheating.

In order to identify the worst dates and times of discomfort glare during the year, 4320 outputs resulted for each position. In total, 17280 outputs are taken for the base model. Although multiple dates and times resulted explicitly for each position, no dates were found that have a discomfort glare in all four positions at the same time. Accordingly, it makes more sense to select dates that have an intolerable glare in at least three positions to have an identical number of dates for comparing the impact of shadings in maximum directions. The simulation outputs show 18 dates (Table A1) that DGP≥0.45 in maximal three positions simultaneously, filtered by Design Explorer and presented in Fig. A1, as in the Appendix. The dates are selected by maximum DGP values in all three positions. Hence, positions facing west (P1), south (P2), and

Fig. 6. Quality of View in the base model. 100% of the test points have view access.

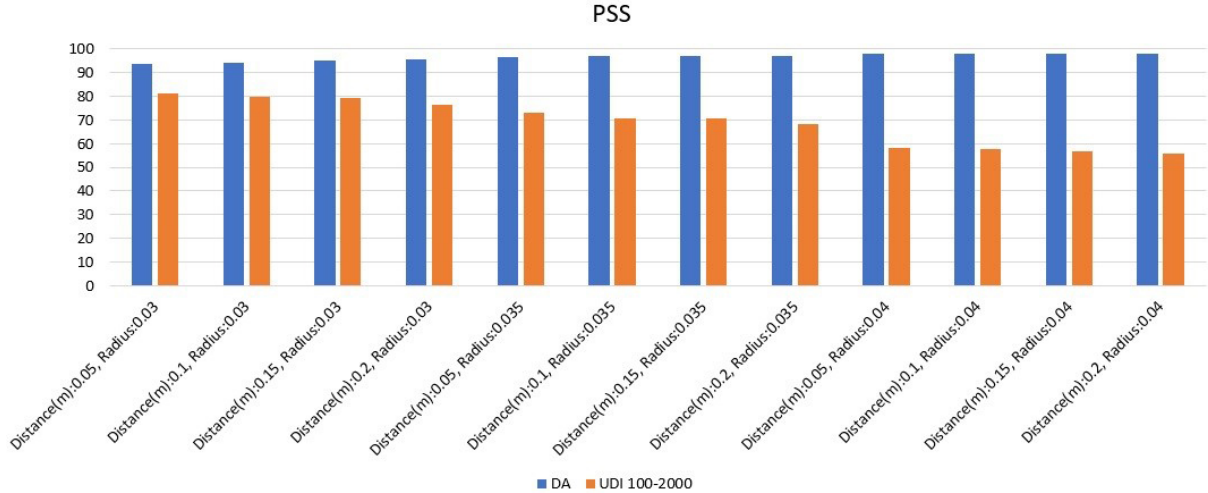

Fig. 7. PSS model's daylight performance. The DA and UDI are based on percentages.

2383-8701/© 2022 The Author(s). Published by solarlits.com. This is an open access article under the CC BY license (https://creativecommons.org/licenses/by/4.0/).

east (P3) are chosen. Figure 5 illustrates some of the DGP results in both FalseColor and Graphics Interchange Format (GIF).

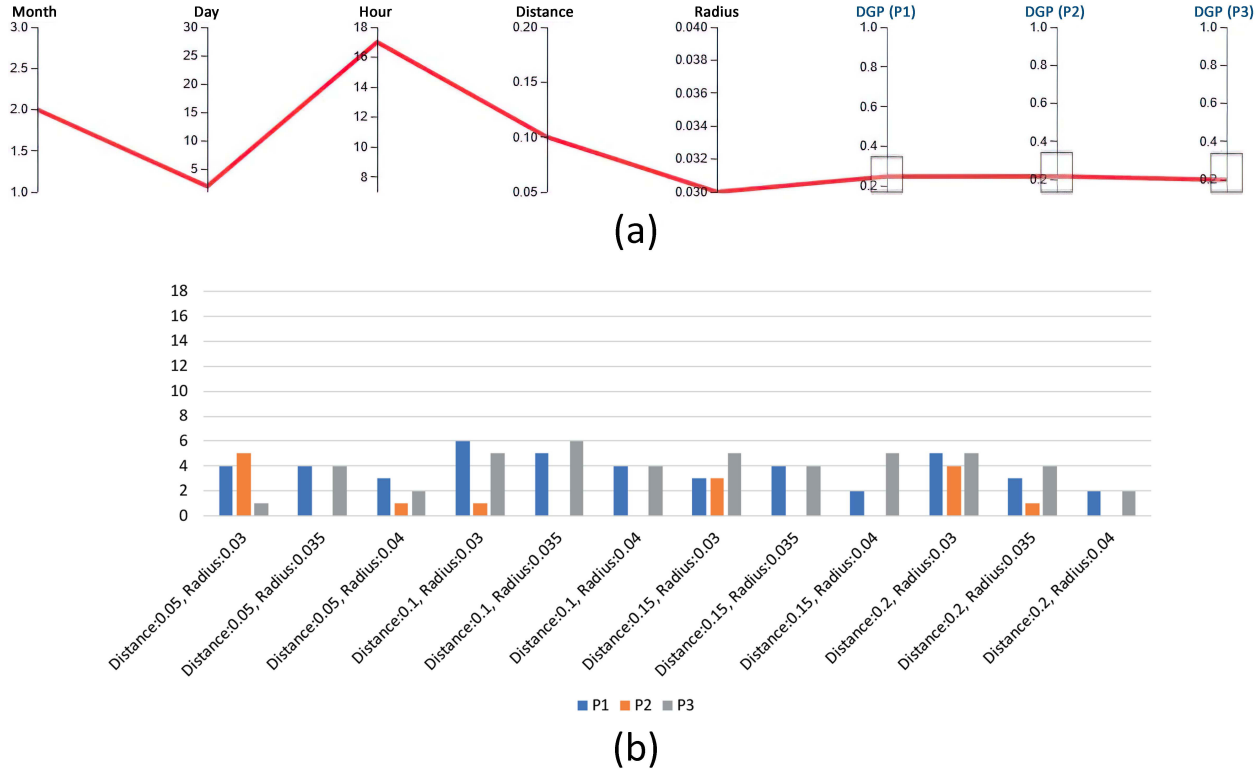

Fig. 8. (**a**) DGP<0.35 simultaneously for three user positions, (**b**) The number of dates that the specific PSS model can reduce discomfort glare for three positions.

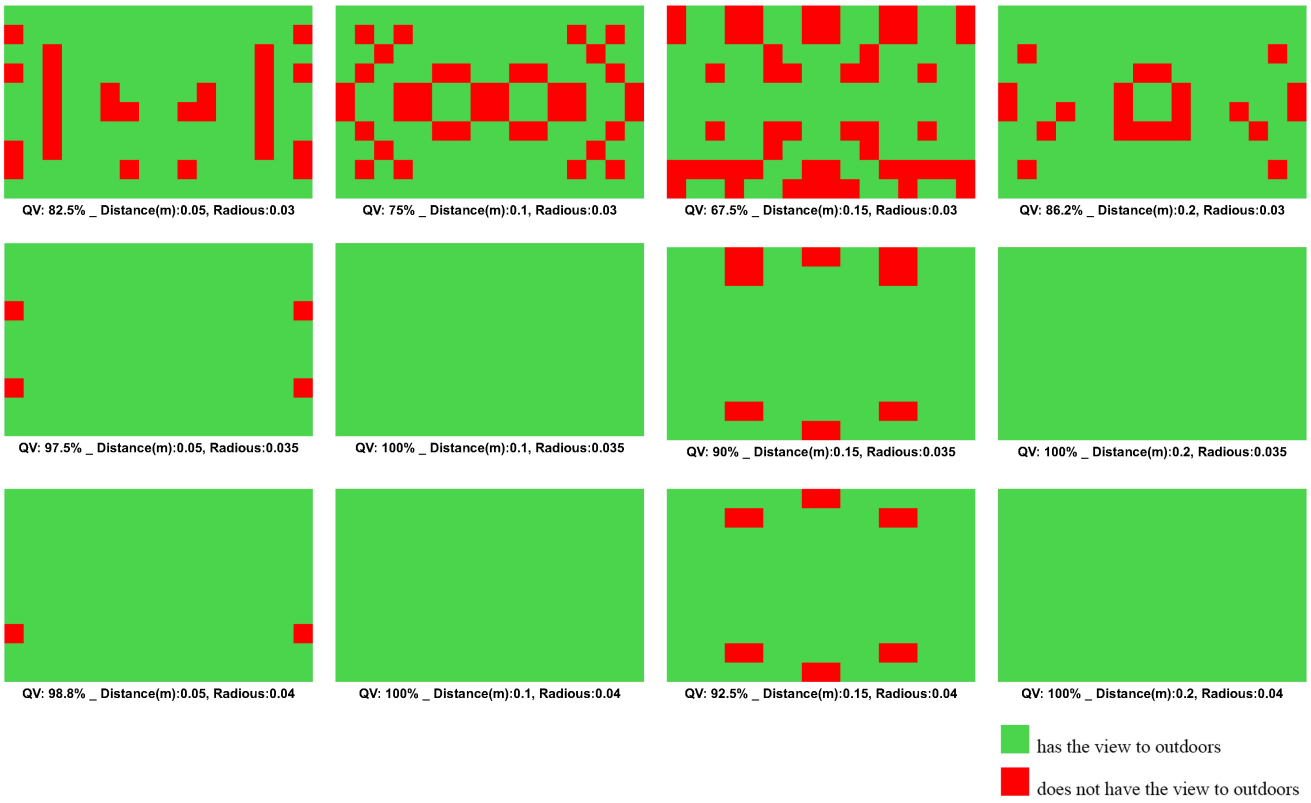

Fig. 9. QV assessment for PSS models. The values above 75% are accepted.

2383-8701/© 2022 The Author(s). Published by solarlits.com. This is an open access article under the CC BY license (https://creativecommons.org/licenses/by/4.0/).

The view analysis output for the base model proves that the points on the view analysis surface have 100% view access to the outdoors based on LEED v4 (Fig. 6).

4.2. Perforated solar screen (PSS)

The possible variations listed in Table 2 are investigated. In total, 12 modes are simulated for the PSS device in the Annual Daylight Simulation. As Fig. 7 illustrates, the PSS keeps the DA at an acceptable level even with the lowest perforation ratio percentage (the smallest circle radius). On the other hand, UDI decreases as the radius of the circle increases and vice versa. Even at their lowest rate, the UDI values are higher than the base model. No significant effect on DA and UDI in varying the glass measurement distance is observed. The lowest UDI (55.71%) and the highest DA (98.08%) can be seen at a distance of 20cm from the glass and a radius of 4cm. Also, the highest UDI (81.40%) and the lowest DA (93.55%) occur at a distance of 5cm from the glass and a radius of 3cm.

Glare analysis proves that given all three positions have a DGP<0.35 simultaneously, the PSS can hold the range on one date, where the shade is located at a distance of 10cm from the glass and a radius of 3cm (Fig. 8(a)). Regarding system specifications that contain the most dates, Fig. 8(b) demonstrates that PSS reduces glare for P3 on six dates when the distance to glass is 10cm, and the radius is 3.5cm. PSS also helps mitigate glare on five dates for p2, where the radius is 3cm at a 5cm distance to glass. It seems

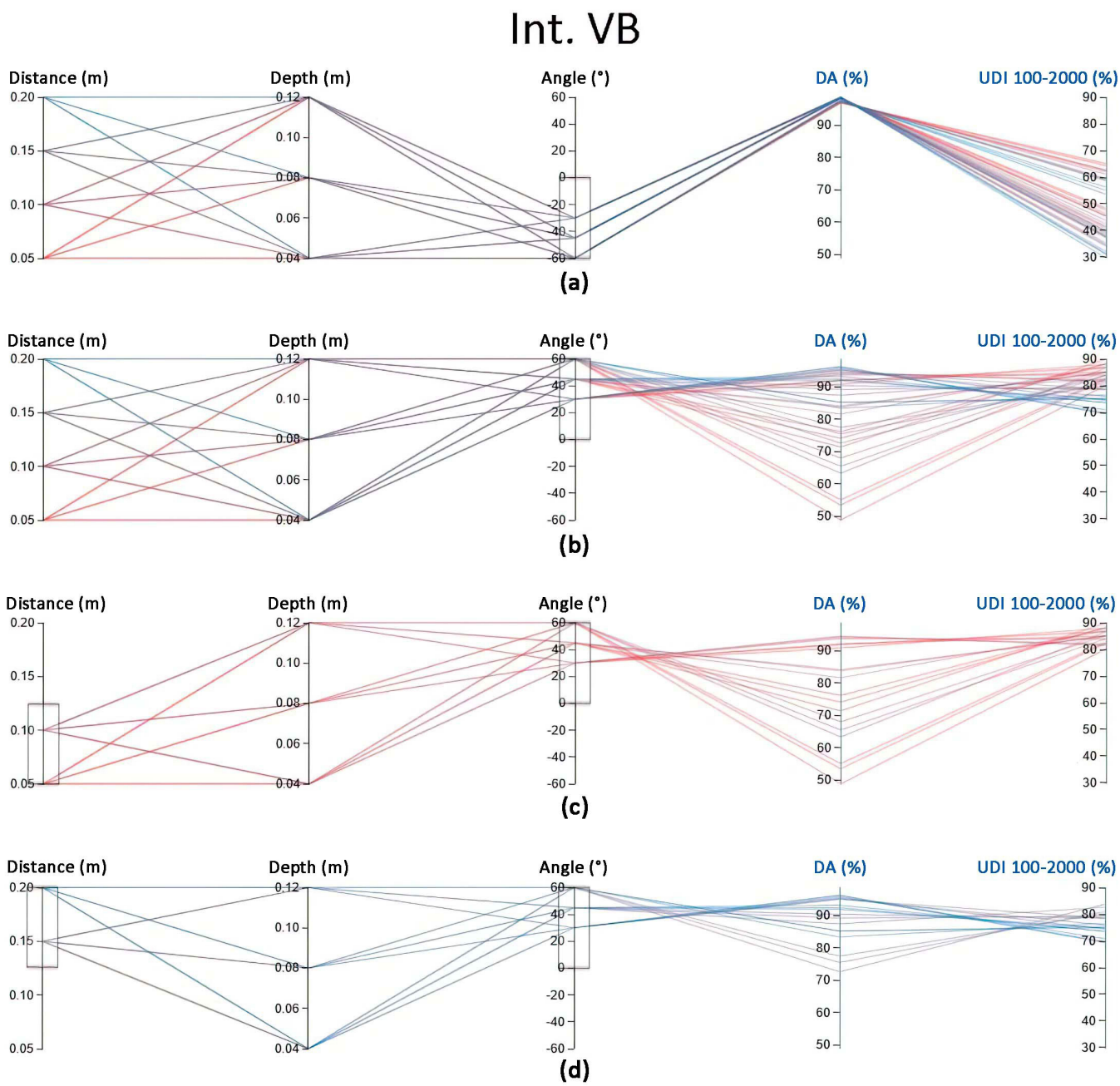

Fig. 10. Daylight performance analysis results of Interior Venetian Blinds, (a): while negative angles are filtered, (b): while positive angles are filtered, (c): while positive angles and long-distance are filtered, and (d): while positive angles and short distance are filtered.

2383-8701/© 2022 The Author(s). Published by solarlits.com. This is an open access article under the CC BY license (https://creativecommons.org/licenses/by/4.0/).

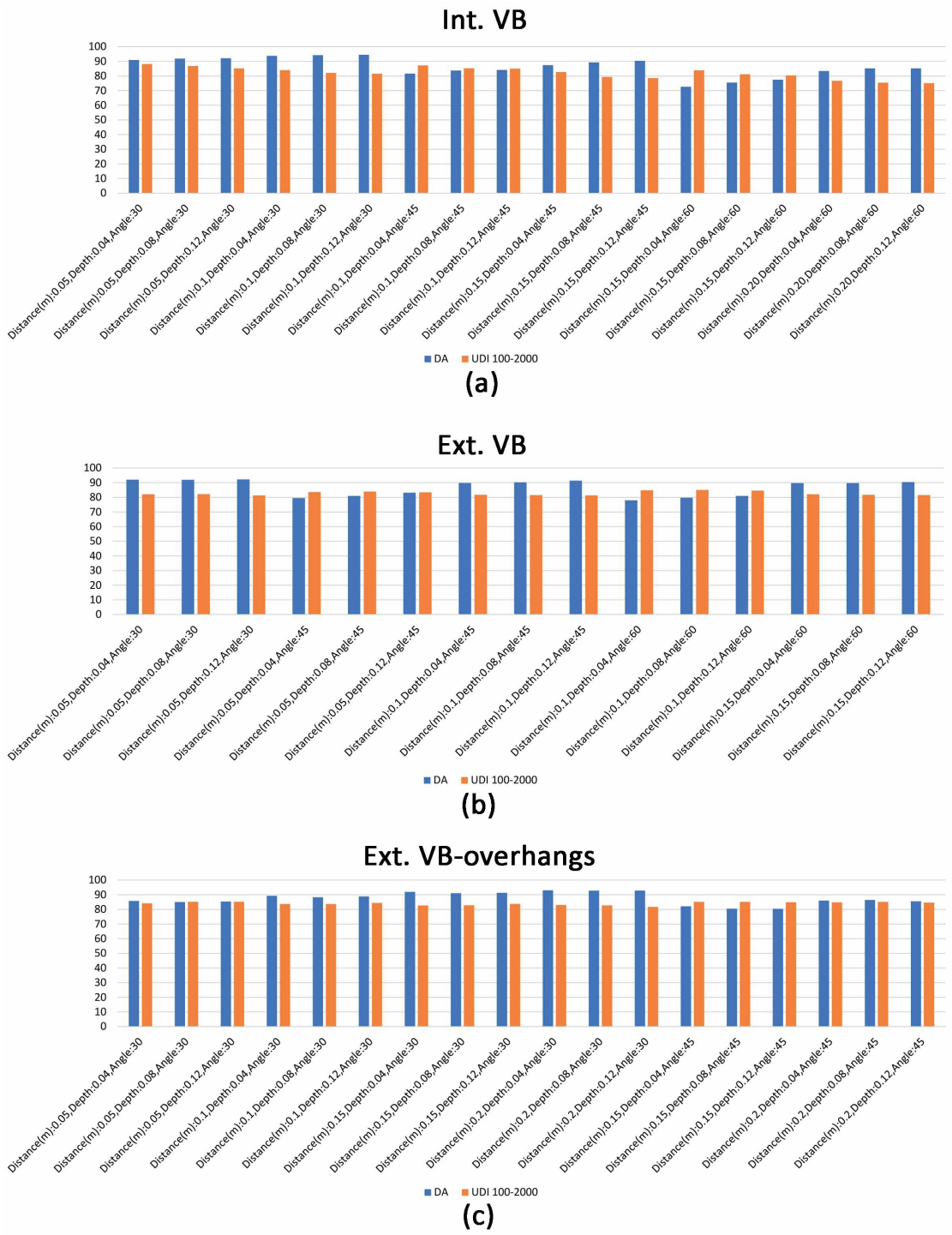

Fig. 11. The DA and UDI values are both in a high border range for (**a**) Int. VB, (**b**) Ext. VB, and (**c**) Ext. VB-overhangs.

that the most critical parameter in reducing glare is radius since the smaller the radius, the better the glare control. It should be noted that although the distance to the glass is not a worthless parameter, it is less valuable than the radius. Given the extent to which PSS has been able to reduce glare, it can be claimed that it has advantages over the base model but still does not meet the goal.

As Fig. 9 reports, in general, QV is in the PSS models in favorable conditions. However, a 3cm radius meets the view only if the distance is 5cm or 20cm. The rest of the models are desirable in any radius and distance. Radius is the most substantial factor yet again in this simulation. Moreover, it seems that distance is not an insignificant factor since, at the distance of 15cm, QV is at the lowest value (Fig. A2).

4.3. Interior venetian blinds (Int. VB)

Figure 10 presents daylight performance for this shading. As Fig. 10(a) depicts, negative angles are not fruitful in increasing the UDI values in the range of 100-2000. However, they are superior to the base model. It can be seen from Fig. 10(b) that positive angles are in pleasant condition. Considering the positive angles, the longer

2383-8701/© 2022 The Author(s). Published by solarlits.com. This is an open access article under the CC BY license (https://creativecommons.org/licenses/by/4.0/).

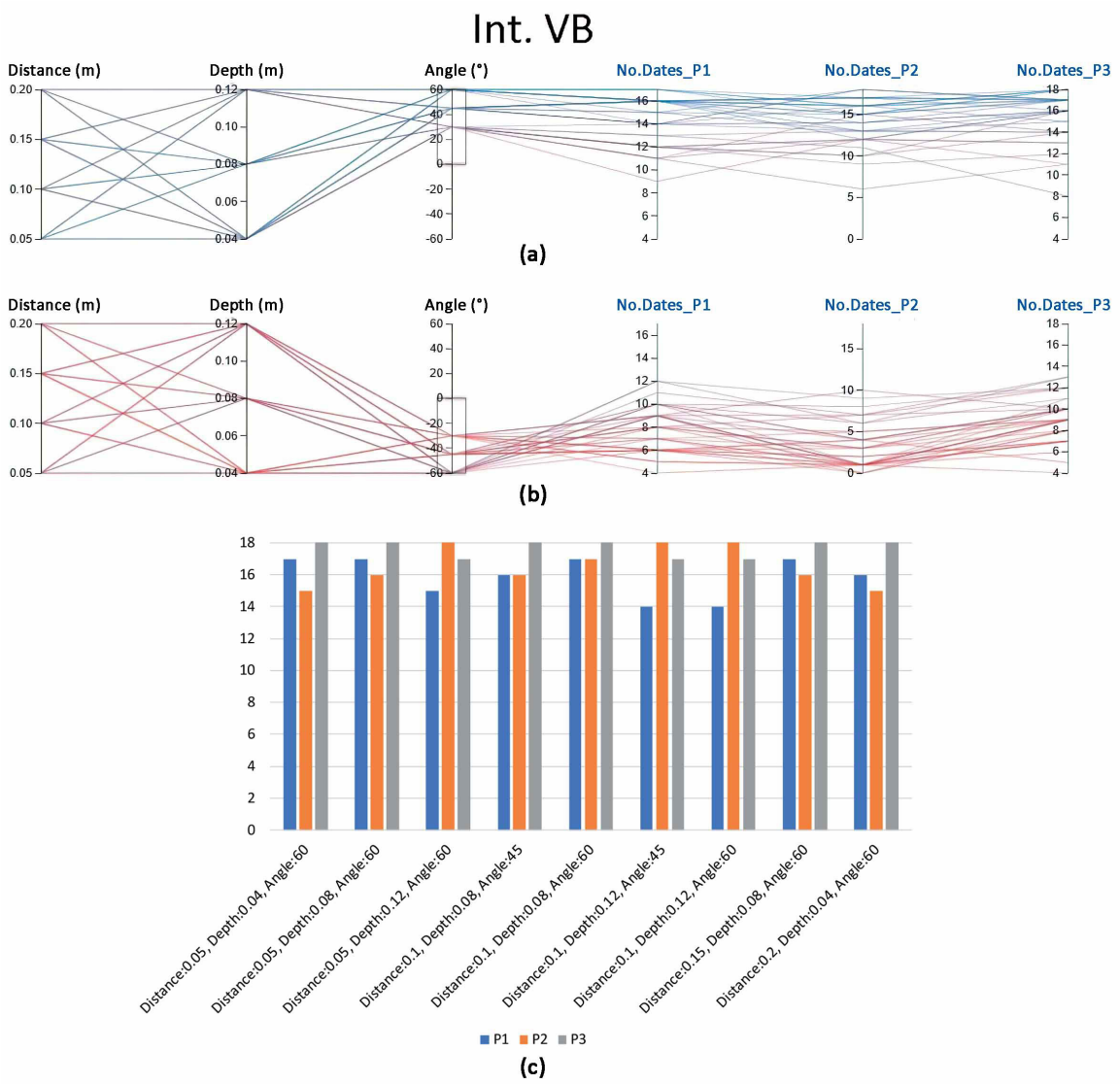

Fig. 12. The number of dates in which the Interior Venetian Blinds can reduce discomfort glare (DGP<0.35) (**a**) while positive angles are filtered, (**b**) while negative angles are filtered, and (**c**) specifications of the shading with DGP <0.35 for each position on most dates.

distance to the glass, the greater the DA value (Fig. 10(c)), and the shorter distances, the lower the DA value (Fig. 10(d)), whereas this situation is reverse for UDI. The slats at +60° and +45° significantly reduce DA but increase UDI values. Nevertheless, at an angle of +30°, an enhancement of DA values is observed compared to positive angles. It is noteworthy that there are cases where both the DA and UDI values are within a high and border range which has occurred at angles of +30°, +45°, and +60° with all depths and specific distances (Fig. 11(a)). Hence, the most influential variables are the angle and the distance to glass, respectively. However, the slats' depth is not an insignificant factor since, at +60° and +45° with a distance of 20cm, the depth of 4cm, compared to the other depths, a tangible reduction in DA value is perceived. The lowest UDI value is 29.5% at -30°, 20cm distance to glass, and 12cm slats' depth, while the highest is 90.1% in +45°, 5cm distance, and 4cm depth, respectively. The DA at the maximum values is in the negative slats' angle, especially -30°, whereas the minimum value is 48.8% at +60° with 5cm away from the glass and a depth of 4cm.

As Fig. 12 reports the number of dates on which the shading can control discomfort glare, the correlation is seen between the positive angles and the glare reduction (Fig. 12(a)). In contrast, the result is reversed for negative angles (Fig. 12(b)). In some cases, it is observed that -30° does not include any date, resulting in the worst angle for P2. As Fig. 13 displays, it turns out that among the positive angles, +60° performs well, while +30° has a poorer performance. No cases are detected under the condition where all three positions are controlled simultaneously on 18 dates synchronously. Although +60° and +45° also perform well for P1, neither can prevent glare on 18 dates, and only 17 dates are supported for this position in some cases where the angles are +60°. If the shading is placed with 12cm slats' depth, +60° angle, and 5 or 10cm distance to glass, as well as at +45° and 10cm distance to glass, P2 could be safe from discomfort glare on 18 dates. According to the above results, it seems that the slats' depth is the second priority of the influential parameter to reduce glare. As it can be interpreted from the Figure, P2 and P3 have better

2383-8701/© 2022 The Author(s). Published by solarlits.com. This is an open access article under the CC BY license (https://creativecommons.org/licenses/by/4.0/).

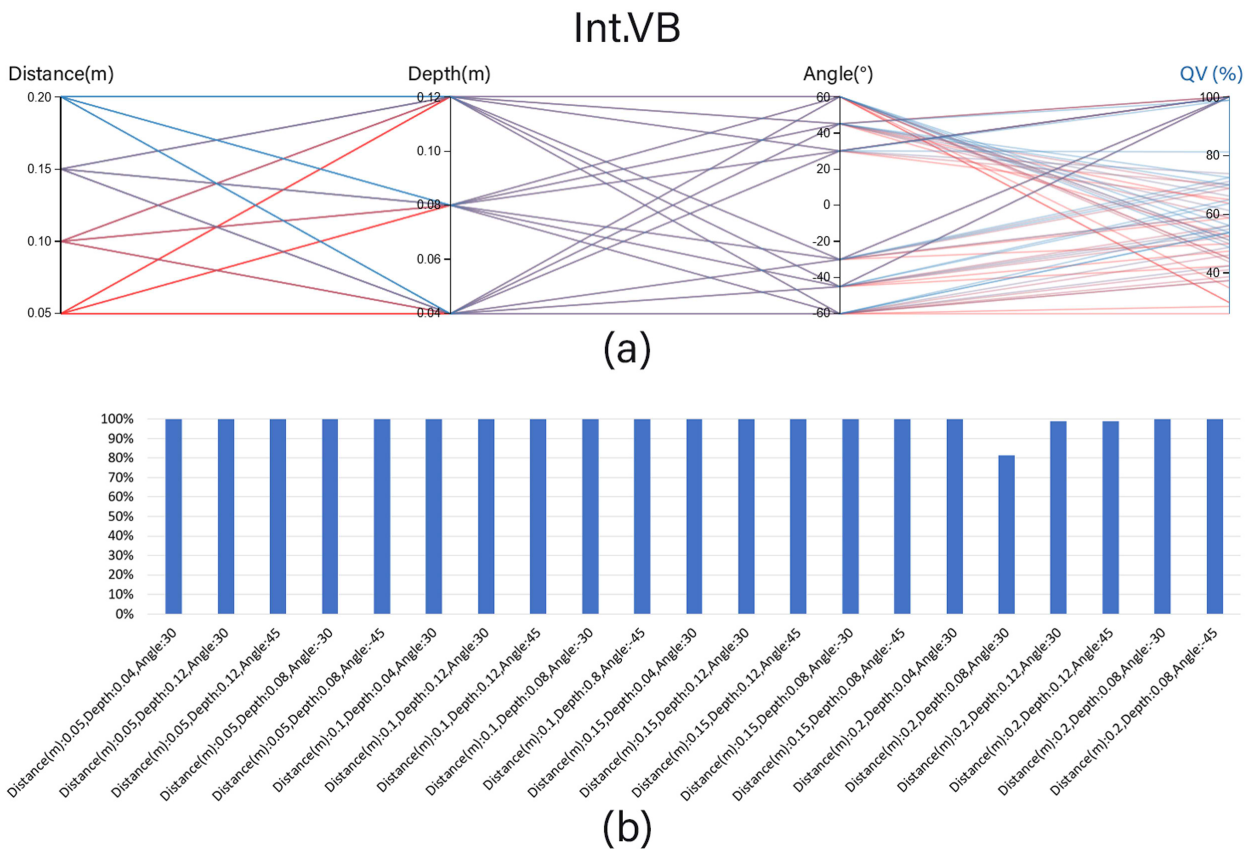

Fig. 13. (**a**) QV assessment results and (**b**) The cases pass the LEED v4 for Interior Venetian Blinds.

conditions for this shading as it gets rich in negating uncomfortable glare on 18 dates.

It can be perceived from Fig. 13(a) that angle also plays a crucial role in view analysis. It is realized that the angle of 60°, neither positive nor negative is competent since QV is less than 75%. Although a meaningful association between slats' depth and QV is not found, the depth parameter is also effective. For the reason that the angle of -30° works only with the depth of 8cm in all the distances and has acceptable results (Fig. 13(b)). Accordingly, +45° only with 12cm depth, -45° with 8cm depth and +30° with 4cm as well as 12cm depth have excellent performance. An exception in +30°, the distance of 20cm and a depth of 8cm are found, which also performs well. Thus, 21 cases can pass the LEED v4.

4.4. Exterior venetian blinds (Ext. VB)

As Fig. 14 demonstrates, negative slats' angle results for Ext. VB in increasing DA values but having low efficiency for UDI values (Fig. 14(a)). Among the positive angles, +60° is less effective in intensifying DA while playing a substantial role in increasing UDI (Fig. 14(b)). However, compared to the previous model, DA values increase significantly at +60° and +45°. At the lowest value, UDI is 33.3%, where the shading is placed at -30° with 20cm distance to glass and 12cm depth, while the highest value is 85% at +60° with 10cm distance and 8cm depth. The DA value in the worst condition is 58.8% at +60° with a distance of 5cm to glass and 4cm depth, whereas the greatest is in the negative angles, in particular -30°. As Fig. 14(c) and (d) shows, the significance of distance to the glass measurements in daylight performance is noticeable, similar to the previous model results. Cases that set the daylight performance values at the appropriate level are presented in Fig. 11(b), which happens at angles of +30°, +45°, and +60° with all depths and particular distances.

As Fig. 15 clarifies, compared to the previous model, the results of the angles aimed at dealing with the glare problem are reversed. The positive angles do not perform well in achieving this goal (Fig. 15(a)). However, negative angles are not adequate to reduce glare for 18 dates as much as the Int. VB (Fig. 15(b)). It can be perceived from the Figure that -60° and -45° have the best performance, whereas the +30° and +45° angles have the worst.

Due to the maximum date that the shading keeps DGP<0.35 in P1, Fig. 15(c) reports 17 dates when the distance to glass is 15cm, the depth of slats is 8cm, and the angle of -60° while in P2, 15 dates resulted where the depth is 4, and the distance is 15cm. The shading in P3 can get 15 dates in 4cm depth with 5cm. Therefore, P1 is introduced as the ideal position for Ext. VB. Aiming to diminish glare, similar to Int. VB, depth also results in a second influential parameter.

Regarding QV assessment, as with the previous shading, the lack of proper performance of the 60° angles, whether positive or negative, can be realized in Fig. 16(a). On the contrary to Int. VB model, the selected cases based on meeting LEED v4, are in symmetrical angles but in the same depths Fig. 16(b). The other difference is also attributed to the number of cases that satisfy LEED v4, in which 20 cases are found in this shading.

2383-8701/© 2022 The Author(s). Published by solarlits.com. This is an open access article under the CC BY license (https://creativecommons.org/licenses/by/4.0/).

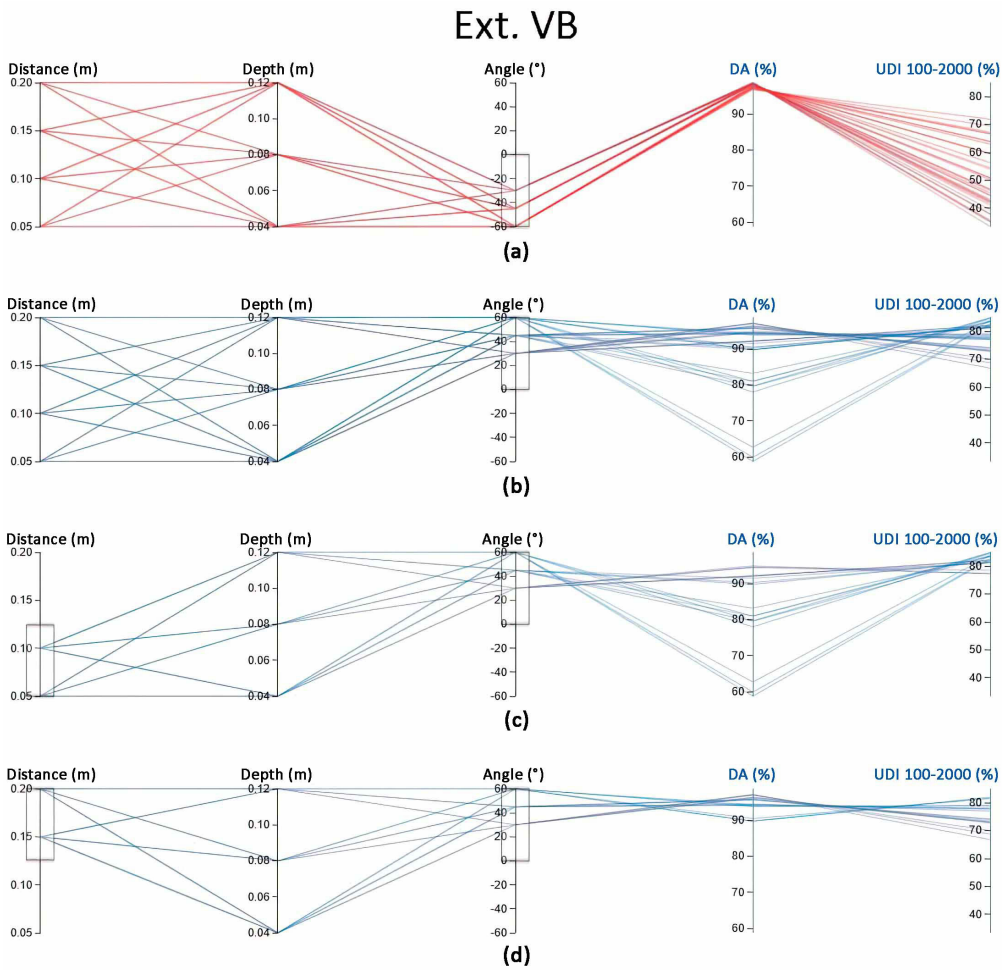

Fig. 14. Daylight performance analysis results of Exterior Venetian Blinds, (**a**) while negative angles are filtered, (**b**) while positive angles are filtered, (**c**) while positive angles and long-distance are filtered, and (**d**) while positive angles and short distance are filtered.

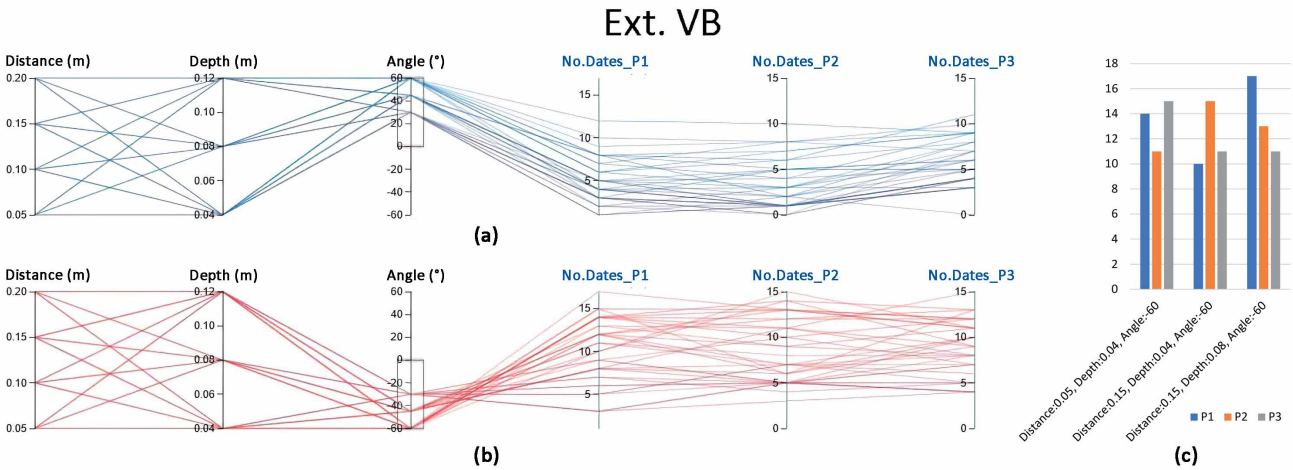

Fig. 15. The number of dates in which the Exterior Venetian Blinds can reduce discomfort glare (DGP<0.35) (**a**) while positive angles are filtered, (**b**) while negative angles are filtered, and (**c**) specifications of the shading with DGP <0.35 for each position on most dates.

4.5. Exterior Venetian Blinds integrated with overhangs (Ext. VB-overhangs).

Results verify that similar to Ext. VB, the slats' angle, is introduced as the most significant parameter in daylight performance and glare reduction. In this case, it also can be stated that the negative angles perform well in intensifying DA values, specifically -30° (Fig. 17(a)). However, contrary to the previous model, in this shading, +60° and +45° diminish DA values sharply while increasing UDI very slightly (Fig. 17(b)). Except for the mentioned angles, the intensity of the tendency to increase the UDI values at all the angles is greater than the Ext. VB, whereas the reduction in DA is less noticeable. The lowest UDI values

2383-8701/© 2022 The Author(s). Published by solarlits.com. This is an open access article under the CC BY license (https://creativecommons.org/licenses/by/4.0/).

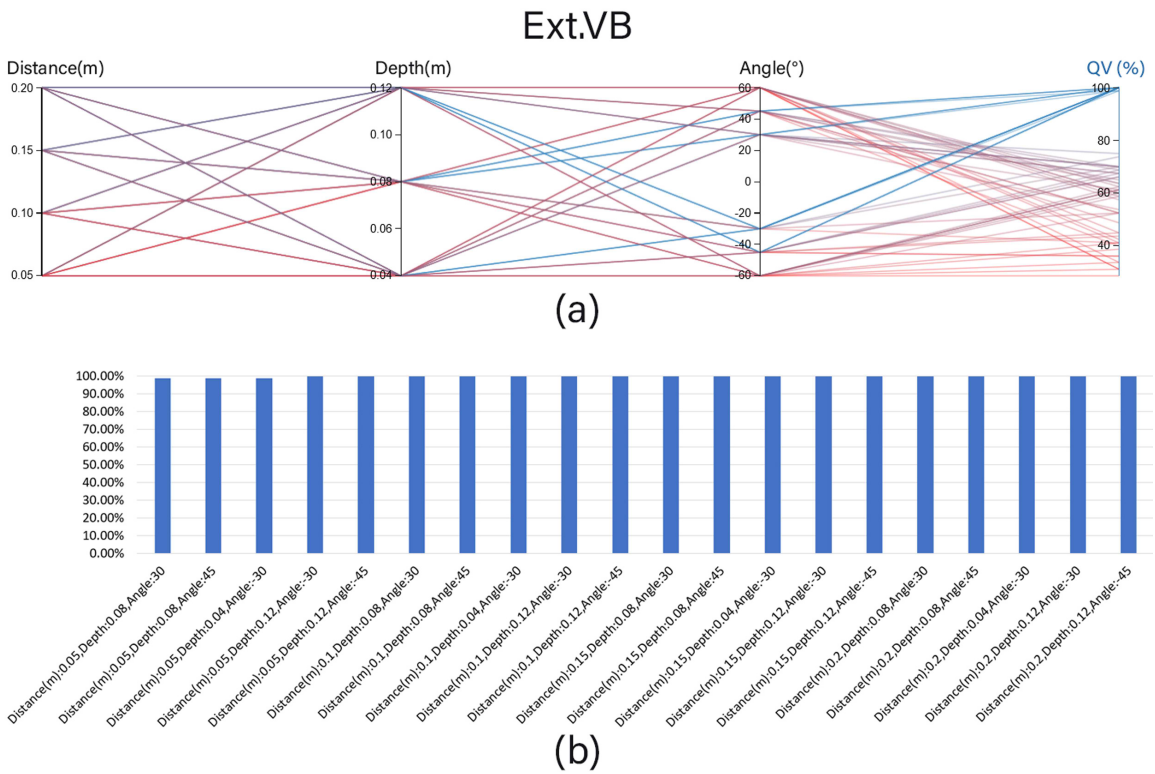

Fig. 16. (**a**) QV assessment results and (**b**) The cases pass the LEED v4 for Exterior Venetian Blinds.

occur at -30°, and the bottommost is 50.7% in 15cm distance with 4cm depth, whereas the most are 87.1% at +60°, with a distance of 20cm and a depth of 8cm, respectively. The lowest DA value is assessed at 38.3% in +60°, 12cm slats' depth, and 5cm distance to glass, whereas the maximum values are at -30°, -45°, and -60° angles, respectively. As Fig. 17(c) and (d) demonstrates, similar to previous models, a shorter distance to glass leads to an intensification of UDI values and a diminution of DA value, and vice versa. Therefore, the results make this parameter more substantial. The range in which DA and UDI both are befitting includes all +30° besides 45° with all depths and particular distances, which can be observed in Fig. 11(c).

Due to the result drawn from glare analysis, it turns out that there are no cases involving 18 dates, as Fig. 18 presents. Similar to the previous blinds, the angle of +30° has the worst function, especially for P2 (Fig. 18(b)). The significant angle is -60° (Fig. 18(a)). As Fig. 18(c) reveals, based on the maximum date that each position could achieve the goal, P1 is supported on 16 dates, whereas P2 is safe on 15 dates in some models with angles of -60° and -45°. The poor performance of this shading for P3 is evident in the figure as it supports only 13 dates.

As Fig. 19(a) demonstrates, QV analysis outputs prove that the results are consistent with the previous shading, while Ext. VB-overhangs model is less inclined to be accepted in LEED v4. The same models meet LEED. As a result, 20 models are presented in Fig. 19(b).

5. Discussion

The results presented in the previous section show some variances between applied shadings to enhance daylight and visual comfort. Figures 7, 10, 14, and 17 give information about the number of DA and UDI simulation models. Although many studies have been carried out on PSS in the background, which claimed that the perforation ratio is effective in both energy and daylight performance, in addition to confirming this tip relates to daylight (Fig. 7), the effect of this parameter in reducing glare has also been identified (Fig. 8). As the Figure clarifies, the smaller the radius, the better the glare control. There is no sensible correlation between the distance to glass neither on glare diminution, nor daylight efficiency. Therefore, the most influential factor is the radius in glare reduction. Besides, some models can provide the quality of view for the occupants depending on the aperture radius (Fig. 9). Remarkably, the shade distance to the glass is not a worthless parameter for QV. Although the PSS model enjoys relatively keeping dynamic daylight performance metrics at a proportional level, no results are found to reduce glare into a comfortable range on all 18 dates. In the best performance, it covers only six dates. Hence it follows that the PSS is practically inappropriate aim at glare reduction throughout the year compared to different Blinds typologies.

The previous studies found that the angle and distance of blinds to glass play a key role in daylight efficiency. This study affirms their findings for all the mentioned types of blinds since the practical results are derived from the angle and distance classification, while the data are almost the same at all slats' depths (Fig. 11). As another reason to prove it, if Figs. 10, 14, and 17 are examined, it can be observed that the shortest distance to glass leads to the lowest DA, and the most extended distances increase DA. Nonetheless, this study goes beyond these results, intended to assess glare and the quality of the view. It is revealed that the angles and slats' depths are substantial in dealing with glare problems, respectively. Although no meaningful relationship is

2383-8701/© 2022 The Author(s). Published by solarlits.com. This is an open access article under the CC BY license (https://creativecommons.org/licenses/by/4.0/).

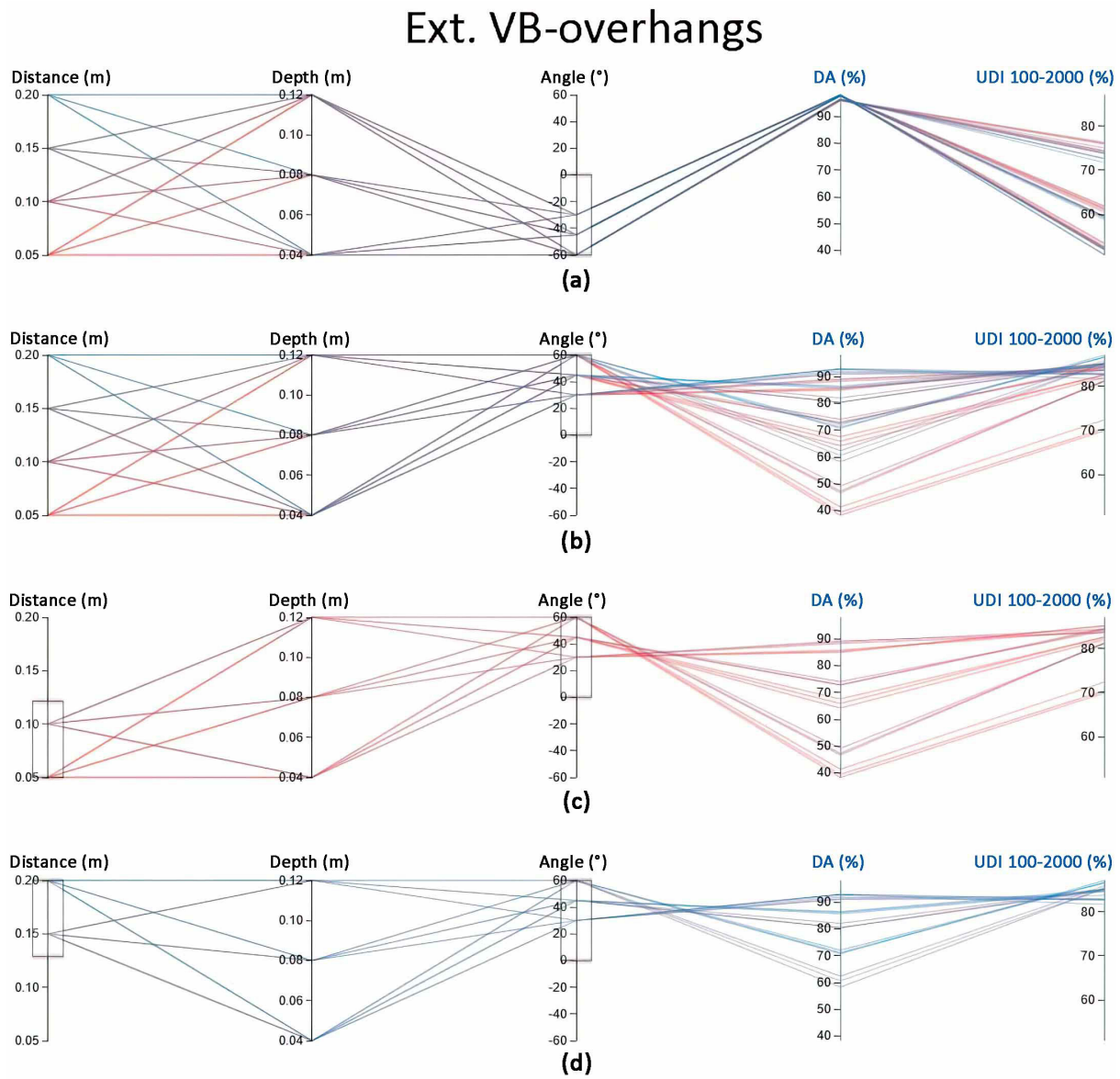

Fig. 17. Daylight performance analysis results of Exterior Venetian Blinds integrated with overhangs, (**a**) while negative angles are filtered, (**b**) while positive angles are filtered, (**c**) while positive angles and long-distance are filtered, and (**d**) while positive angles and short distance are filtered.

observed, discomfort glare decreases at specific depths. In addition, it is determined that the angle also affects the quality of view, which is a chief factor in visual comfort. Even though no noticeable correlation is found between slats' depth and quality of view, its effect on QV is undeniable. The results in the blinds are very similar, and the only negligible difference is whether the shading is external or internal, considering the negative or positive angle with the specific depth of the slats to meet the LEED v4.

Given the background, the comparison of blinds inside and outside the building was less compared in terms of visual comfort, while in this article, the superiority of Int. VB resulted. Owing to the slats' angles' deformation inside and outside (Fig. 3 (b.1), (b.2), and (c.1)), it predicted that the results would be reversed for the inner and outer blinds. Nonetheless, the results are also dissimilar in symmetrical angles, probably due to whether they are external or internal. As Figs. 12 and 15 show, positive angles outperform the negative in Int. VB, whereas for Ext. VB, positive angles have better function than the negative, but not sufficient to achieve the glare reduction. It can be affirmed that the performance of Ext. VB, according to the respective position, is not as pleasant as Int. VB. However, Ext. VB is still beneficial.

Among the various studied Blinds typologies, there was no study on the Ext. VB-overhangs in which it is found that overhangs that are integrated with this shading compared to the simple model could have little effect on reducing glare risks and daylight performance. The results between Ext. VB and Ext. VB-overhangs are relatively similar. Notwithstanding the resemblances between Ext. VB-overhangs and Ext. VB, it can be declared that Ext. VB-overhangs underperform Ext. VB. In previous studies, the shadings were usually evaluated on one side of the building. In contrast, this study concludes that even if the shadings are located on all four sides of the building, there is a growing tendency for useful daylight to be more within the acceptable range. The high potential of blinds performance is also

2383-8701/© 2022 The Author(s). Published by solarlits.com. This is an open access article under the CC BY license (https://creativecommons.org/licenses/by/4.0/).

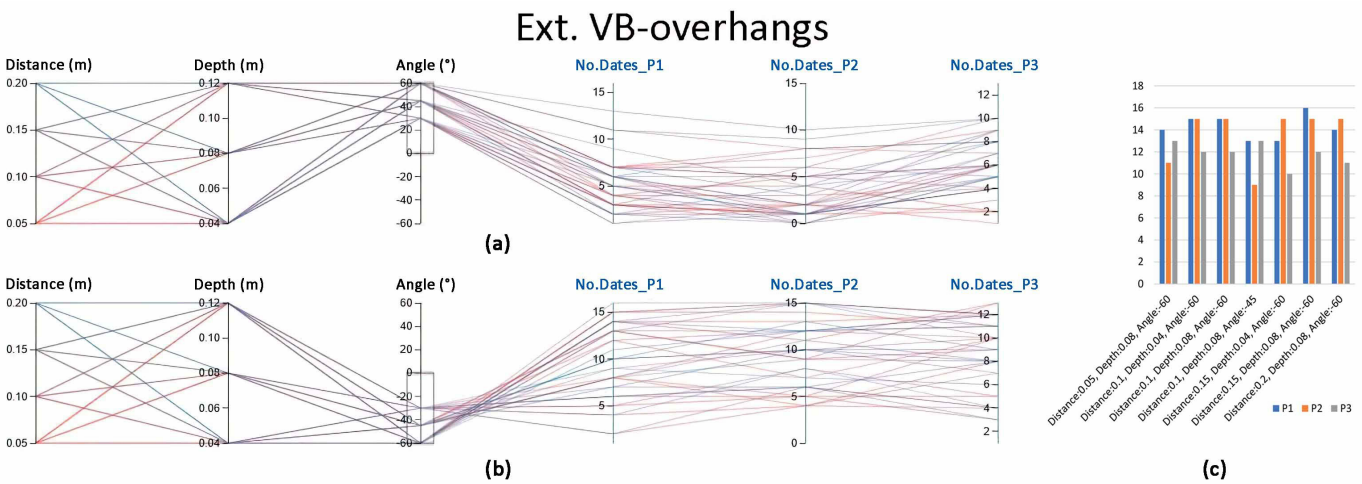

Fig. 18. The number of dates in which the Exterior Venetian Blinds integrated with overhangs can reduce discomfort glare (DGP<0.35) (**a**) while positive angles are filtered, (**b**) while negative angles are filtered, and (**c**) specifications of the shading with DGP <0.35 for each position on most dates.

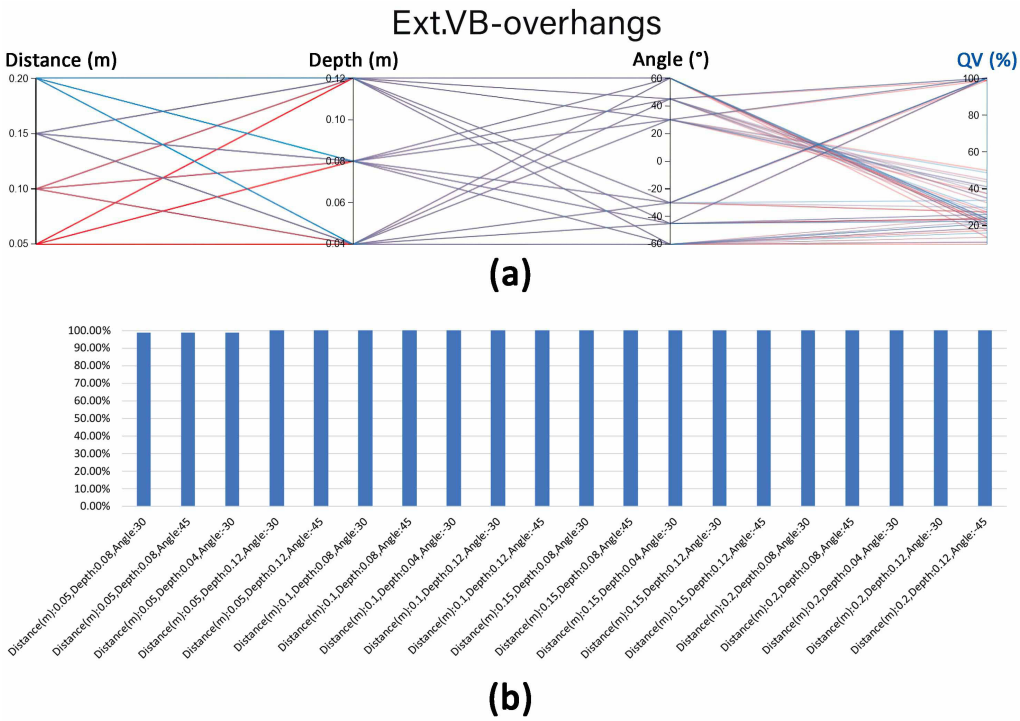

Fig. 19. (**a**) QV assessment results and (**b**) The cases pass the LEED v4 for Exterior Venetian Blinds integrated with overhangs.

revealed with the aim of glare decrement on all four sides of the room throughout the year. However, it is found that Int. VB in the south and east has a more beneficial effect on glare control, while external blinds are more successful in the west because the user is safe from glare on more dates in these directions. The recommended user positions for each shading are summarized in Table A2 in the Appendix.

Although the shading devices need to be optimized, at this stage of the study, it can be stated that some PSS models can probably improve the efficiency of useful daylight up to 5.4 times while it can only reduce glare by about 33%. In this regard, considering the models with the average DA higher than 50%, Int. VB improves the useful daylight about six times and eliminates glare depending on the angle and the user's field of view. This claim for Ext. VB and Ext. VB-overhangs are close to 5.6 and 5.7, respectively, and 94% and 88% for glare control.

To sum up briefly, if only daylight performance is considered, the PSS seems to be a reasonable shade. If, in addition to the daylight performance, a discomfort glare alleviation is intended, Int. VB can be introduced as the supreme shading among the studied shadings. In the second and third priority, Ext. VB and Ext. VB-overhangs are recommended, respectively. Accordingly, since not much difference is observed between the blinds in QV, the Int. VB can be preferred in terms of daylight efficiency, reduced glare, and the quality of the view.

Due to the long time-consuming simulation, this study had limitations. Given that the angle is introduced as an essential factor, more angles could be simulated to determine the exact shading

2383-8701/© 2022 The Author(s). Published by solarlits.com. This is an open access article under the CC BY license (https://creativecommons.org/licenses/by/4.0/).

angle to achieve the goals. Moreover, several critical glare phenomena may have been missed by the hourly time steps to be detected for glare simulation. Besides, to have an ideal reading room, the effect of the shadings on the natural ventilation and thermal comfort needs to be studied. It is hoped that future studies will fill these gaps.

6. Conclusions

Aligning with the current studies that necessitate daylight performance analysis combined with visual comfort, the present study proposes improvements considering a reading room in four directions openings to deal with glare problems, quality of view, and daylight enhancement. Four shading devices were simulated to clarify the role of each in increasing daylight performance and visual comfort. Except for a 60-min time step throughout the year to determine the worst dates and times, about 12312 daylight glare simulations, 229 cases for annual daylight metrics, and 229 cases for view analysis were evaluated. Insufficient glare mitigation as a result of applying the PSS model was found in this study, while the propensity to increase daylight performance was evident. Perforation radius was the most impressive parameter in achieving the goal. Daylight performance in satisfaction ranges was reported for the different blinds, and the most serious variables were the slats' angle and the distance to the glass, respectively. No meaningful relevance was evidenced for blinds' distance to the glass to deal with the glare problem, but sensible effectiveness was observed for slats' depth. Generally, compared to the base model, all the shading devices made the UDI more in the appropriate range. Although the DA was lower than the base model, cases were still in the acceptable range.

Regarding enhancing daylight performance for blinds, similarities were seen. In terms of diminishing glare, it can be concluded that Int. VB outperformed the other devices. Concerning Quality of View, it was perceived that there were models in PSS and the blinds which pass LEED v4 due to their aperture radius and the angle of slats, respectively. Notably, the slats' depth was also a significant factor for blinds to achieve view access. This study's findings could lead designers to make decisions for similar buildings with comparable climate conditions and latitudes.

Nevertheless, it is essential to state that the results were based on a limited number of studied variable parameters, which took a long time to simulate each case. Other proper, various window-to-wall ratio ranges, more variable parameters for shading devices, various time-steps, external obstructions, and different climatic conditions should be investigated. It is believed that these factors can be assessed through further studies. There is a need for data analysis to be optimized to find out which one resulted in both minimizing discomfort glare and maximizing annual daylight simultaneously. Therefore, a further step of this research will be carried out to optimize the authors' cases in a future study.

Appendix

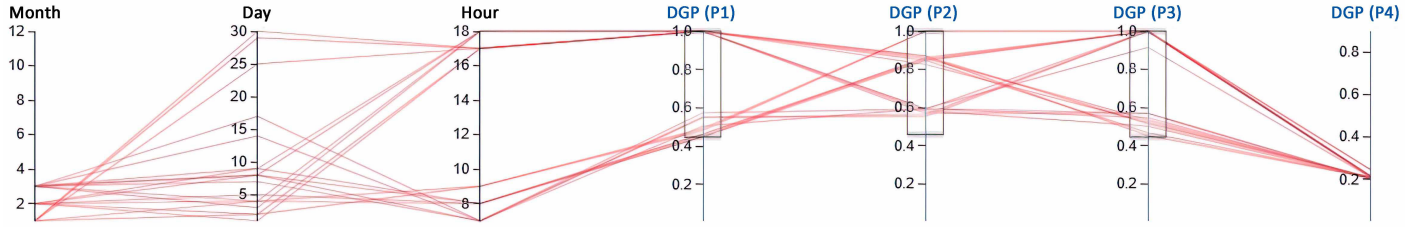

Fig. A1. DGP analysis with 60-min time step throughout the year in four positions.

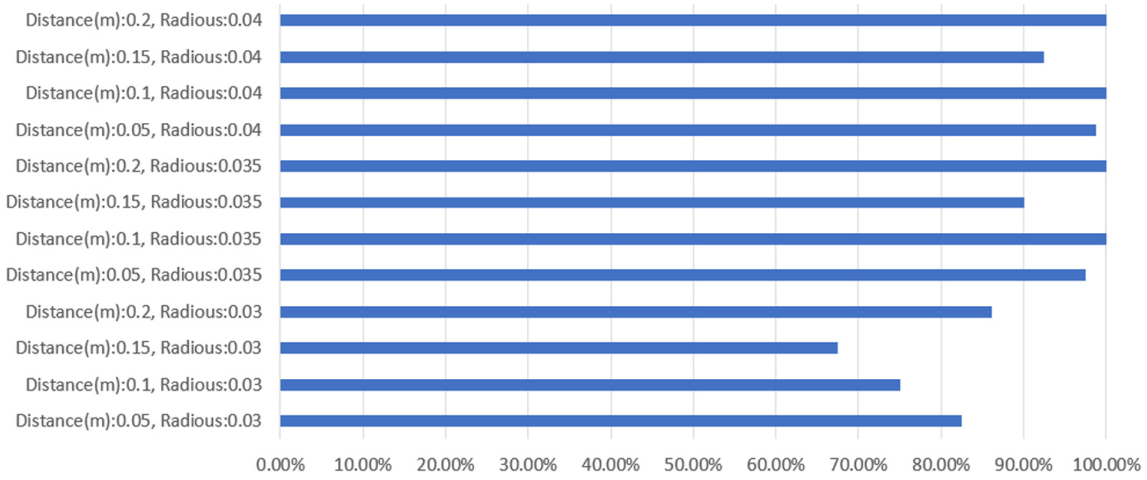

Fig. A2. QV assessment for PSS models. The values above 75% are accepted.

2383-8701/© 2022 The Author(s). Published by solarlits.com. This is an open access article under the CC BY license (https://creativecommons.org/licenses/by/4.0/).

Table A1. The worst dates and times of discomfort glare (one-hour time step from 7 am to 6 pm throughout the year).

	Month	Day	Hour	DGP (P1)	DGP (P2)	DGP (P3)	DGP (P4)
1	1	2	9	0.48	1	1	0.24
2	1	4	9	0.50	1	1	0.32
3	1	25	17	1	0.86	0.45	0.20
4	1	29	17	1	0.85	0.54	0.26
5	1	30	17	1	0.86	0.52	0.26
6	2	4	8	0.45	0.86	1	0.21
7	2	5	8	0.46	0.85	1	0.21
8	2	8	8	0.46	0.85	1	0.21
9	2	1	17	1	0.87	0.47	0.25
10	2	2	17	1	0.84	0.46	0.20
11	3	7	7	0.55	0.60	1	0.25
12	3	8	7	0.49	0.60	1	0.25
13	3	14	7	0.56	0.56	1	0.25
14	3	17	7	0.57	0.56	1	0.25
15	3	3	18	1	0.57	0.56	0.23
16	3	4	18	1	0.59	0.56	0.23
17	3	8	18	1	0.59	0.55	0.23
18	3	9	18	1	0.58	0.57	0.23

Table A2. Recommended positions and shadings based on the maximum dates with a DGP <0.35.

Shading type	Specifications	Position	Number of supported dates
PSS	Distance: 0.1, Radius: 0.03	Facing west (P1)	6
	Distance: 0.1, Radius: 0.0.35	Facing west (P3)	
Int. VB	Distance: 0.05, Depth: 0.04, Angle: 60	Facing east (P3)	18
	Distance: 0.05, Depth: 0.08, Angle: 60		
	Distance: 0.1, Depth: 0.08, Angle: 45		
	Distance: 0.1, Depth: 0.08, Angle: 60		
	Distance: 0.15, Depth: 0.08, Angle: 60		
	Distance: 0.2, Depth: 0.04, Angle: 60		
Int. VB	Distance: 0.05, Depth: 0.12, Angle: 60	Facing south (P2)	18
	Distance: 0.1, Depth: 0.12, Angle: 45		
	Distance: 0.10, Depth: 0.12, Angle: 60		
Ext.VB	Distance: 0.15, Depth: 0.08, Angle: -60	Facing south (P1)	17
Ext.VB_Overhangs	Distance: 0.15, Depth: 0.08, Angle: -60	Facing south (P1)	16

Contributions

B. Dabaj contributes conceptualization, methodology, software, formal analysis, investigation, writing- original draft preparation, visualization. M. Rahbar (corresponding author) contributes validation, writing- reviewing and editing, supervision, project administration, funding acquisition. B. V. Fakhr contributes validation, resources, writing- reviewing and editing, data curation, project administration.

Declaration of competing interest

The authors declare no conflict of interest.

References

[1] L. Heschong, Windows and classrooms: A study of student performance and the indoor environment, California Energy Commission 37 (2003) 414-435.

[2] A. Tzempelikos, Advances on daylighting and visual comfort research, Building and environment 100 (2017) 1-4.

[3] S. M. Hosseini, M. Mohammadi, A. Rosemann, T. Schröder, and J. Lichtenberg, A morphological approach for kinetic façade design process to improve visual and thermal comfort, Building and Environment 153 (2019) 186-204.

[4] Q. Yao, W. Cai, M. Li, Z. Hu, P. Xue, and Q. Dai, Efficient circadian daylighting: A proposed equation, experimental validation, and the consequent importance of room surface reflectance, Energy and Buildings 210 (2020) 109784.

[5] P. Stone, The effects of environmental illumination on melatonin, bodily rhythms and mood states: a review, International Journal of Lighting Research and Technology 31 (1999) 71-79.

[6] L. Doulos, A. Tsangrassoulis, and F. Topalis, Quantifying energy savings in daylight responsive systems: The role of dimming electronic ballasts, Energy and Buildings 40 (2008) 36-50.

[7] S. Bunjongjit and A. Ngaopitakkul, Feasibility study and impact of daylight on illumination control for Energy-saving lighting systems, Sustainability 10 (2018) 4075.

[8] J. Y. Suk, M. Schiler, and K. Kensek, Development of new daylight glare analysis methodology using absolute glare factor and relative glare factor, Energy and Buildings 64 (2013) 113-122.

[9] I. E. S. O. N. America, Lighting handbook: Reference & application, Illuminating Engineering Society of North America, 2000.

[10] W. K. Osterhaus, Discomfort glare assessment and prevention for daylight applications in office environments, Solar Energy 79 (2005) 140-158.

[11] L. Heschong, Daylighting and Human Performance, ASHRAE Journal (2002) 65-67.

2383-8701/© 2022 The Author(s). Published by solarlits.com. This is an open access article under the CC BY license (https://creativecommons.org/licenses/by/4.0/).

[12] J. H. Heerwagen and G. H. Orians, Adaptations to windowlessness: A study of the use of visual decor in windowed and windowless offices, Environment and Behavior 18 (1986) 623-639.
[13] T. Hwang and J. T. Kim, Effects of indoor lighting on occupants' visual comfort and eye health in a green building, Indoor and Built Environment 20 (2011) 75-90.
[14] J. Y. Suk, M. Schiler, and K. Kensek, Investigation of existing discomfort glare indices using human subject study data, Building and Environment 113 (2017) 121-130.
[15] S. M. Hosseini, M. Mohammadi, and O. Guerra-Santin, Interactive kinetic façade: Improving visual comfort based on dynamic daylight and occupant's positions by 2D and 3D shape changes, Building and Environment 165 (2019) 106396.
[16] E. S. Saunders, University of Paris Libraries: Sainte Genevieve Library, Libraries Research Publications (2001) 24.
[17] S. de Neumann, Oodi-Helsinki Central Library: Making the architectural vision a reality, ce/papers 3 (2019) 157-164.
[18] L. Ray and K. V. Macy, Assessment in space designed for experimentation, The University of Washington libraries research commons (2014).
[19] I. Acosta, M. Á. Campano, R. Leslie, and L. Radetsky, Daylighting design for healthy environments: Analysis of educational spaces for optimal circadian stimulus, Solar Energy 193 (2019) 584-596.
[20] T. J. Dabe and V. S. Adane, The impact of building profiles on the performance of daylight and indoor temperatures in low-rise residential building for the hot and dry climatic zones, Building and Environment 140 (2018) 173-183.
[21] M. Lu and J. Du, Dynamic evaluation of daylight availability in a highly-dense Chinese residential area with a cold climate, Energy and Buildings 193 (2019) 139-159.
[22] C. W. Kwon and K. J. Lee, Integrated daylighting design by combining passive method with daysim in a classroom, Energies 11 (2018) 3168.
[23] I. Acosta, M. Á. Campano, S. Domínguez-Amarillo, and C. Muñoz, Dynamic daylight metrics for electricity savings in offices: Window size and climate smart lighting management, Energies 11 (2018) 3143.
[24] N. Abdollahzadeh, M. Tahsildoost, and Z. S. Zomorodian, A method of partition design for open-plan offices based on daylight performance evaluation, Journal of Building Engineering 29 (2020) 101171.
[25] F. Fathy, Y. Mansour, H. Sabry, M. Refat, and A. Wagdy, Conceptual framework for daylighting and facade design in museums and exhibition spaces, Solar Energy 204 (2020) 673-682.
[26] A. P. de Almeida Rocha, G. Reynoso-Meza, R. C. Oliveira, and N. Mendes, A pixel counting based method for designing shading devices in buildings considering energy efficiency, daylight use and fading protection, Applied Energy 262 (2020) 114497.
[27] M. Salamati, P. Mathur, G. Kamyabjou, and K. Taghizade, Daylight performance analysis of TiO2@ W-VO2 thermochromic smart glazing in office buildings, Building and Environment 186 (2020) 107351.
[28] W. El-Abd, B. Kamel, M. Afify, and M. Dorra, Assessment of skylight design configurations on daylighting performance in shopping malls: A case study, Solar Energy 170 (2018) 358-368.
[29] B. Abboushi, I. Elzeyadi, K. Van Den Wymelenberg, R. Taylor, M. Sereno, and G. Jacobsen, Assessing the visual comfort, visual interest of sunlight patterns, and view quality under different window conditions in an open-plan office, LEUKOS 17 (2020) 321-337.
[30] J. Y. Garretón, A. M. Villalba, R. G. Rodriguez, and A. Pattini, Roller blinds characterization assessing discomfort glare, view outside and useful daylight illuminance with the sun in the field of view, Solar Energy 213 (2021) 91-101.
[31] P. Pilechiha, M. Mahdavinejad, F. P. Rahimian, P. Carnemolla, and S. Seyedzadeh, Multi-objective optimisation framework for designing office windows: quality of view, daylight and energy efficiency, Applied Energy 261 (2020) 114356.
[32] M. Kim, I. Konstantzos, and A. Tzempelikos, Real-time daylight glare control using a low-cost, window-mounted HDRI sensor, Building and Environment 177 (2020) 106912.
[33] Y. Bian, Q. Dai, Y. Ma, and L. Liu, Variable set points of glare control strategy for side-lit spaces: Daylight glare tolerance by time of day, Solar Energy 201 (2020) 268-278.
[34] R. Wang, G. Li, L. Xu, Y. Wang, and C. Peng, Integration of sun-tracking shading panels into window system towards maximum energy saving and non-glare daylighting, Applied Energy 260 (2020) 114304.
[35] N. Kunwar, K. S. Cetin, U. Passe, X. Zhou, and Y. Li, Full-scale experimental testing of integrated dynamically-operated roller shades and lighting in perimeter office spaces, Solar Energy 186 (2019) 17-28.
[36] Y. Bian, T. Leng, and Y. Ma, A proposed discomfort glare evaluation method based on the concept of'adaptive zone', Building and Environment 143 (2018) 306-317.
[37] P. Xue, Q. Li, J. Xie, M. Zhao, and J. Liu, Optimization of window-to-wall ratio with sunshades in China low latitude region considering daylighting and energy saving requirements, Applied Energy 233 (2019) 62-70.
[38] Y. Fang and S. Cho, Design optimization of building geometry and fenestration for daylighting and energy performance, Solar Energy 191 (2019) 7-18.
[39] T. Srisamranrungruang and K. Hiyama, Balancing of natural ventilation, daylight, thermal effect for a building with double-skin perforated facade (DSPF), Energy and Buildings 210 (2020) 109765.
[40] S. Lu, B. Lin, and C. Wang, Investigation on the potential of improving daylight efficiency of office buildings by curved facade optimization, Building Simulation 13 (2020) 287-303.
[41] H. Kim and M. J. Clayton, A multi-objective optimization approach for climate-adaptive building envelope design using parametric behavior maps, Building and Environment 185 (2020) 107292.
[42] M. Pesenti, G. Masera, and F. Fiorito, Exploration of adaptive origami shading concepts through integrated dynamic simulations, Journal of Architectural Engineering 24 (2018) 04018022.
[43] A. Tabadkani, M. V. Shoubi, F. Soflaei, and S. Banihashemi, Integrated parametric design of adaptive facades for user's visual comfort, Automation in Construction 106 (2019) 102857.
[44] B. Bueno, J. M. Cejudo-López, A. Katsifaraki, and H. R. Wilson, A systematic workflow for retrofitting office façades with large window-to-wall ratios based on automatic control and building simulations, Building and Environment 132 (2018) 104-113.
[45] D. Uribe, W. Bustamante, and S. Vera, Potential of perforated exterior louvers to improve the comfort and energy performance of an office space in different climates, Building Simulation 11 (2018) 695-708.
[46] F. Nicoletti, C. Carpino, M. A. Cucumo, and N. Arcuri, The Control of Venetian Blinds: A Solution for Reduction of Energy Consumption Preserving Visual Comfort, Energies 13 (2020) 1731.
[47] D. Uribe, S. Vera, W. Bustamante, A. McNeil, and G. Flamant, Impact of different control strategies of perforated curved louvers on the visual comfort and energy consumption of office buildings in different climates, Solar Energy 190 (2019) 495-510.
[48] S. Samadi, E. Noorzai, L. O. Beltrán, and S. Abbasi, A computational approach for achieving optimum daylight inside buildings through automated kinetic shading systems, Frontiers of Architectural Research 9 (2020) 335-349.
[49] L. Santos, A. Leitão, and L. Caldas, A comparison of two light-redirecting fenestration systems using a modified modeling technique for Radiance 3-phase method simulations, Solar energy 161 (2018) 47-63.
[50] Y. Tan et al., Parametric study of venetian blinds for energy performance evaluation and classification in residential buildings, Energy 239 (2022) 122266.
[51] H. Huo, W. Xu, A. Li, J. Chu, and Y. Lv, Sensitivity analysis and prediction of shading effect of external Venetian blind for nearly zero-energy buildings in China, Journal of Building Engineering 41 (2021) 102401.
[52] Y. Tyukhova and C. Waters, Subjective and pupil responses to discomfort glare from small, high-luminance light sources, Lighting Research & Technology 51 (2019) 592-611.
[53] Z. Hamedani et al., Visual discomfort and glare assessment in office environments: A review of light-induced physiological and perceptual responses, Building and Environment 153 (2019) 267-280.
[54] Z. Hamedani, E. Solgi, T. Hine, and H. Skates, Revealing the relationships between luminous environment characteristics and physiological, ocular and performance measures: An experimental study, Building and Environment 172 (2020) 106702.
[55] Z. Hamedani, E. Solgi, T. Hine, H. Skates, G. Isoardi, and R. Fernando, Lighting for work: A study of the relationships among discomfort glare, physiological responses and visual performance, Building and Environment 167 (2020) 106478.
[56] M. Rosenfield, Computer vision syndrome: a review of ocular causes and potential treatments, Ophthalmic and Physiological Optics 31 (2011) 502-515.
[57] H. Byrd, Post-occupancy evaluation of green buildings: the measured impact of over-glazing, Architectural Science Review 55 (2012) 206-212.
[58] S. Yigit, A machine-learning-based method for thermal design optimization of residential buildings in highly urbanized areas of Turkey, Journal of Building Engineering 38 (2021) 102225.

2383-8701/© 2022 The Author(s). Published by solarlits.com. This is an open access article under the CC BY license (https://creativecommons.org/licenses/by/4.0/).

[59] J. Ngarambe, A. Irakoze, G. Y. Yun, and G. Kim, Comparative performance of machine learning algorithms in the prediction of indoor daylight illuminances, Sustainability 12 (2020) 4471.

[60] R. W. da Fonseca, F. O. Pereira, and K. Papamichael, The potential of artificial neural networks to model daylight harvesting in buildings located in different climate zones, in: Proceedings of the 15th International Building Performance Simulation Association Conference, 2017, pp. 2103-2112.

[61] E. Brembilla, D. Chi, C. Hopfe, and J. Mardaljevic, Evaluation of climate-based daylighting techniques for complex fenestration and shading systems, Energy and Buildings 203, (2019) 109454.

[62] C. F. Reinhart, J. Mardaljevic, and Z. Rogers, Dynamic daylight performance metrics for sustainable building design, Leukos 3 (2006) 7-31.

[63] Z. Keskin, Y. Chen, and S. Fotios, Daylight and seating preference in open-plan library spaces, International Journal of Sustainable Lighting 17 (2015) 12-20.

[64] A. Michael and C. Heracleous, Assessment of natural lighting performance and visual comfort of educational architecture in Southern Europe: The case of typical educational school premises in Cyprus, Energy and Buildings 140 (2017) 443-457.

[65] A. Jovanović, P. Pejić, S. Djorić-Veljković, J. Karamarković, and M. Djelić, Importance of building orientation in determining daylighting quality in student dorm rooms: Physical and simulated daylighting parameters' values compared to subjective survey results, Energy and Buildings 77 (2014) 158-170.

[66] C. F. Reinhart and J. Wienold, The daylighting dashboard-A simulation-based design analysis for daylit spaces, Building and environment 46 (2011) 386-396.

[67] C. Reinhart and O. Walkenhorst, Dynamic RADIANCE-based Daylight Simulations for a full-scale Test Office with outer Venetian Blinds, Energy & Buildings 33 (2001) 683-697.

[68] S. Carlucci, F. Causone, F. De Rosa, and L. Pagliano, A review of indices for assessing visual comfort with a view to their use in optimization processes to support building integrated design, Renewable and sustainable energy reviews 47 (2015) 1016-1033.

[69] E. CEN, 12464-1 Light and lighting-Lighting of work places-Part 1: Indoor work places, European Committee for Standardization (CEN), Brussels, 2011.

[70] C. F. Reinhart and D. A. Weissman, The daylit area-Correlating architectural student assessments with current and emerging daylight availability metrics, Building and environment 50 (2012) 155-164.

[71] R. A. Mangkuto, M. Rohmah, and A. D. Asri, Design optimisation for window size, orientation, and wall reflectance with regard to various daylight metrics and lighting energy demand: A case study of buildings in the tropics, Applied energy 164 (2016) 211-219.

[72] IES LM 83-12 Approved Method: IES Spatial Daylight Autonomy (sDA) and Annual Sunlight Exposure (ASE), Illuminating Engineering Society, 2012.

[73] J. Wienold, J. Christoffersen, Towards a new daylight glare rating, in: Proceedings of the 10th European Lighting Conference, Lux Europa, Lux EuropaBerlin (DE), 2005, pp. 157-161.

[74] J. Wienold and J. Christoffersen, Evaluation methods and development of a new glare prediction model for daylight environments with the use of CCD cameras, Energy and buildings 38 (2006) 743-757.

2383-8701/© 2022 The Author(s). Published by solarlits.com. This is an open access article under the CC BY license (https://creativecommons.org/licenses/by/4.0/).